Molecular nickel phosphide carbonyl nanoclusters: synthesis, structure and electrochemistry of $[Ni_{11}P(CO)_{18}]^{3-}$ and $[H_{6-n}Ni_{31}P_4(CO)_{39}]^{n-}$ (n = 4,5)

Chiara Capacci,[†] Iacopo Ciabatti,[†] Cristina Femoni,[†] Maria Carmela Iapalucci,[†] Tiziana Funaioli,[‡] Stefano Zacchini,*[†] and Valerio Zanotti[†]

[†] Dipartimento di Chimica Industriale "Toso Montanari", Università di Bologna, Viale Risorgimento 4, I-40136 Bologna. Italy.

[‡] Dipartimento di Chimica e Chimica Industriale, University of Pisa, Via Moruzzi 13, 56124 Pisa, Italy.

ABSTRACT: The reaction of $[NEt_4]_2[Ni_6(CO)_{12}]$ in thf with 0.5 equivalents of PCl_3 afforded the mono-phosphide $[Ni_{11}P(CO)_{18}]^{3-}$, that in turn further reacted with PCl_3 resulting in the tetra-phosphide carbonyl cluster $[HNi_{31}P_4(CO)_{39}]^{5-}$. Alternatively, the latter can be obtained from the reaction of $[NEt_4]_2[Ni_6(CO)_{12}]$ in thf with 0.8-0.9 equivalents of PCl_3. The $[HNi_{31}P_4(CO)_{39}]^{5-}$ penta-anion is reversibly protonated by strong acids affording the $[H_2Ni_{31}P_4(CO)_{39}]^{4-}$ tetra-anion, whereas deprotonation affords the $[Ni_{31}P_4(CO)_{39}]^{6-}$ hexa-anion. The latter is reduced with Na/naphthalene yielding the $[Ni_{31}P_4(CO)_{39}]^{7-}$ hepta-anion. In order to shed light on the poly-hydride nature and redox behavior of these clusters, electrochemical and spectroelectrochemical studies were carried out on $[Ni_{11}P(CO)_{18}]^{3-}$, $[HNi_{31}P_4(CO)_{39}]^{5-}$ and $[H_2Ni_{31}P_4(CO)_{39}]^{4-}$. The reversible formation of the stable $[Ni_{11}P(CO)_{18}]^{4-}$ tetra-anion is demonstrated through the spectroelectrochemical investigation of $[Ni_{11}P(CO)_{18}]^{3-}$. The redox changes of $[HNi_{31}P_4(CO)_{39}]^{5-}$ show features of chemical reversibility and the vibrational spectra in the CO stretching region of the nine redox forms of the cluster $[HNi_{31}P_4(CO)_{39}]^{n-}$ (n = 3 to 11) are reported. The spectroelectrochemical investigation of $[H_2Ni_{31}P_4(CO)_{39}]^{4-}$ revealed the presence of three chemically reversible reductions, and the IR spectra of $[H_2Ni_{31}P_4(CO)_{39}]^{n-}$ (n = 4 to 7) have been recorded. The different spectroelectrochemical behavior of $[HNi_{31}P_4(CO)_{39}]^{5-}$ and $[H_2Ni_{31}P_4(CO)_{39}]^{4-}$ support their formulation as polyhydride. Unfortunately, all the attempts to directly confirm their poly hydrido nature by 1H NMR spectroscopy failed, as previously found for related large metal carbonyl clusters. Thus, the presence and number of hydride ligands have been based on the observed protonation/deprotonation reactions and the spectroelectrochemical experiments. The molecular structures of the new clusters have been determined by single-crystal X-ray analysis. These represent the first examples of structurally characterized molecular nickel carbonyl nanoclusters containing interstitial phosphide atoms.

1. Introduction

Nickel phosphide nanoparticles have recently attracted great interest because of their catalytic properties in reactions such as hydrogenation, hydrodesulfurization (HDS), hydrodeoxygenation (HDO) and hydrodenitrogenation (HDN).[1-3] They also show interesting properties as electrocatalytic materials for the hydrogen evolution reaction (HER).[4-7] Moreover, phosphorus-rich phases such as NiP_2 are promising candidate as reversible lithium-ion battery electrodes.[8]

Nickel forms eight phosphides, *i.e.*, Ni_3P, Ni_5P_2, $Ni_{12}P_5$, Ni_2P, Ni_5P_4, NiP, NiP_2 and NiP_3.[9-13] Ni-rich phases contain isolated P-atoms enclosed within a tricapped trigonal prismatic Ni_9 cage (Ni_2P), a distorted mono-capped square anti-prismatic Ni_9 cage (Ni_3P), a mixture of Ni_{10} sphenocorona and Ni_9 mono-capped cubic cages ($Ni_{12}P_5$). P-P bonds are formed within P-richer phases, resulting in P_2 units (NiP and the high-pressure cubic NiP_2), zig-zig chains (monoclinic NiP_2), P_4 units (NiP_3), as well as more complex and less regular structures.

It has been pointed out that molecular metal nanoclusters might be interesting models for the investigation of metal aggregates at the nanolevel, as well as promising precursors for the preparation of metal nanoparticles and catalytic materials.[14-28] Thus, it is quite remarkable that molecular nickel phosphide nanoclusters have not been reported up to date. This should be contrasted with the tendency of Ni to form several molecular carbonyl clusters containing other fully interstitial p-block elements, such as C, Ga, Ge, Sn, Sb.[25,29] Ni-carbide carbonyl clusters display a very rich chemistry and may contain 1-10 interstitial C-atoms.[30-32] Conversely, heavier hetero-atoms show a poorer chemistry. Ga, Ge and Sn are limited to icosahedral Ni-carbonyl clusters containing a single fully interstitial hetero-atom,[33,34] whereas $[Ni_{11}Bi_2(CO)_{18}]^{3-}$ contains two semi-interstitial Bi-atoms.[35] In the case of Ni-Sb carbonyls, $[Ni_{15}Sb(CO)_{24}]^{2-}$ contains a fully interstitial Sb-atom,[36] whereas semi-interstitial (semiexposed) hetero-atoms are present in $[Ni_{31}Sb_4(CO)_{40}]^{6-}$,[37] $[Ni_{11}Sb_2(CO)_{18}]^{3-}$,[36] $[Ni_{13}Sb_2(CO)_{24}]^{3-}$,[38] $[Ni_{19}Sb_4(CO)_{26}]^{4-}$.[39] In contrast, Zintl type ions containing a few Ni-CO groups have been described, including $[Ni_6Ge_{13}(CO)_5]^{4-}$, $[Ni_7Bi_{12}(CO)_4]^{4-}$, $[Ni_4Bi_3(CO)_6]^{3-}$, $[Ni_4Bi_4(CO)_6]^{3-}$.[40,41] Nickel carbonyl clusters containing E-R (E = Ge, Sn, Sb, Bi; R = organic group) fragments on the surface have been also reported in the literature.[42-44]

Metal carbonyl clusters containing P-atoms are known for Co, Rh, Ru and Os. Because of the larger atomic radius, Os forms the fully interstitial trigonal prismatic $[Os_6P(CO)_{18}]^-$ cluster.[45] Conversely, phosphorus is found within larger square-antiprismatic cages in Ru and Rh clusters, *i.e.*, $[Ru_8P(CO)_{22}]^-$,[46,47] $[Rh_9P(CO)_{21}]^{2-}$, $[Rh_{10}P(CO)_{22}]^{3-}$.[48,49] By further decreasing the metal size, Co-phosphide carbonyls may display either fully interstitial P-atoms, as found in $[Co_9P(CO)_{21}]^{2-}$ (monocapped square-antiprismatic) and $[Co_{10}P(CO)_{22}]^{3-}$ (bicapped square-antiprismatic),[50] or semi-

interstitial phosphides, *i.e.*, $Co_8P_2(CO)_{19}$, $Co_{10}P_2(CO)_{24}$,[51] $[HCo_{10}P_2(CO)_{23}]^{2-}$ [52] and $[Co_6P(CO)_{16}]^-$.[53]

In order to expand our knowledge, we herein report the synthesis and structural characterization of the first molecular nickel phosphide carbonyl nanoclusters, *i.e.* $[Ni_{11}P(CO)_{18}]^{3-}$ and the giant $[H_{6-n}Ni_{31}P_4(CO)_{39}]^{n-}$ (n = 4, 5). The new clusters have been investigated by means of electrochemical and spectroelectrochemical methods, in view of the fact that interstitial heteroatoms are known to confer further stability to metal carbonyl clusters and enhance their propensity towards reversible redox processes.[14,23,25,29,54,55] Nine redox forms of the cluster $[HNi_{31}P_4(CO)_{39}]^{n-}$ (n = 3- 11) have been recognized through spectroelectrochemical experiments and their IR spectra reported. Conversely, the spectroelectrochemical analysis of $[H_2Ni_{31}P_4(CO)_{39}]^{4-}$ reveals only the presence of four differently charged species $[H_2Ni_{31}P_4(CO)_{39}]^{n-}$ (n = 4-7). The different spectroelectrochemical properties of $[HNi_{31}P_4(CO)_{39}]^{5-}$ and $[H_2Ni_{31}P_4(CO)_{39}]^{4-}$, as well as the fact that they can be reversibly interconverted by means of protonation/deprotonation reactions, provide indirect support for the assumption that these clusters have a different number of hydride ligands. The total number of hydrides in each species has been based solely on the number of observed protonation/deprotonation reactions and, therefore, must be taken as a mere hypothesis.

2. Results and Discussion

2.1 Synthesis and molecular structure of $[Ni_{11}P(CO)_{18}]^{3-}$.

The reaction of $[Ni_6(CO)_{12}]^{2-}$ as the $[NEt_4]^+$ salt with 0.5 equivalents of PCl_3 in thf afforded $[NEt_4]_3[Ni_{11}P(CO)_{18}]$ as an oily precipitate. To avoid extensive formation of $Ni(CO)_4$, PCl_3 must be added slowly as a dilute solution in thf. In all cases, traces of $Ni(CO)_4$ (as detected by IR spectroscopy) can be removed under reduced pressure. At the end of the reaction, the precipitate was recovered after filtration, washed with H_2O and thf, and $[Ni_{11}P(CO)_{18}]^{3-}$ was eventually extracted in acetone. Crystals of $[NEt_4]_3[Ni_{11}P(CO)_{18}]$ suitable for X-ray crystallography were grown by slow diffusion of n-hexane into the acetone solution. Formation of $[Ni_{11}P(CO)_{18}]^{3-}$ under these conditions can be accounted for by:

$$2[Ni_6(CO)_{12}]^{2-} + PCl_3 \rightarrow [Ni_{11}P(CO)_{18}]^{3-} + 3Cl^- + Ni^{2+} + 6CO \quad (1)$$

Crystals of $[NEt_4]_3[Ni_{11}P(CO)_{18}]$ display ν(CO) at 1980(s), 1845(m) cm^{-1} in CH_3CN solution. The molecular structure of $[Ni_{11}P(CO)_{18}]^{3-}$ was determined as its $[NEt_4]_3[Ni_{11}P(CO)_{18}]$ salt (Figure 1 and Table 1). The metal cage of the cluster can be described as a mono-capped

sphenocorona (Johnson solid J86) centered by the unique P-atom.[56] The sphenocorona is a solid with idealized C_{2v} symmetry, composed of 10 vertices, 22 edges, 12 triangular and 2 square faces. There are 92 polyhedra which are known as Johnson solids. They were named by Norman Johnson, who first listed them in 1966 (see ref 56). Johnson solids are strictly convex polyhedra that have regular faces but are not uniform (that is, they are not Platonic solids, Archimedean solids, prisms, or antiprisms). The sphenocorona is the 86th polyhedron in the list of Johnson; therefore, it is referred to as J86. It is composed of 10 vertices, 22 edges, and 14 faces (12 triangular and 2 square faces). The idealized symmetry is C_{2v}. The additional Ni atom is capping one of the triangular faces, and is not bonded to the interstitial phosphide. Thus, the P-atom displays a coordination of 10. Alternatively, the $Ni_{11}P$ cage can be viewed as a prism with a square and a pentagonal base, the latter capped by a further Ni-atom resulting in a pentagonal pyramid. The 11th Ni atom is capping one of the triangular faces of the pentagonal pyramid. .

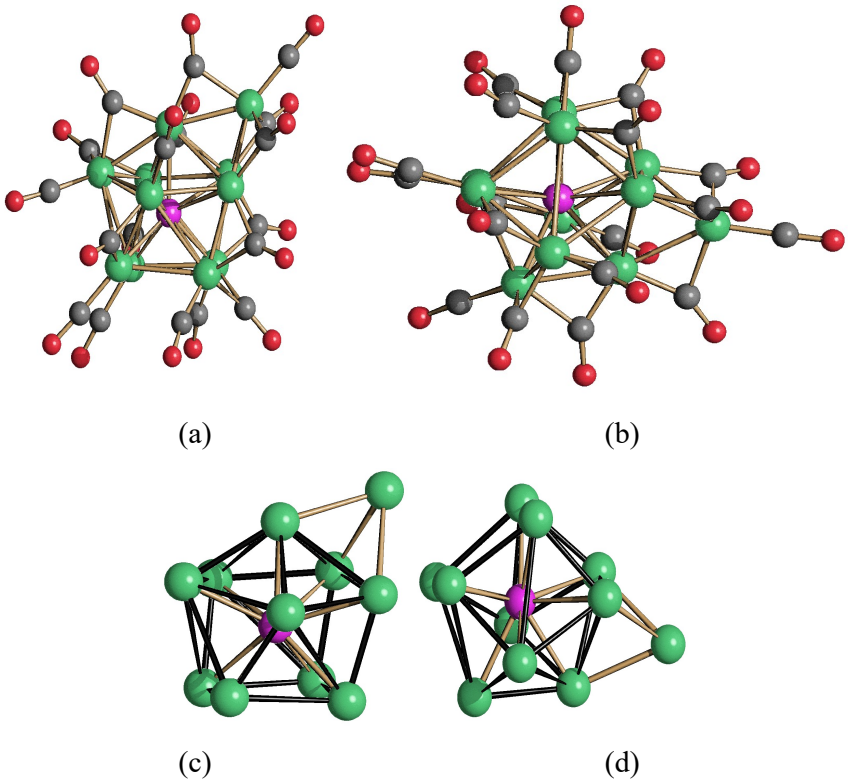

Figure 1. Two different views of (a,b) the molecular structure of $[Ni_{11}P(CO)_{18}]^{3-}$ and (c,d) its $Ni_{11}P$ core (Ni, green; P, purple; C, grey; O, red). The Ni-Ni bonds of the Ni_{10} sphenocorona are represented in black in (c,d).

Table 1. Main bond distances and contacts (Å) of $[Ni_{11}P(CO)_{18}]^{3-}$, $[H_2Ni_{31}P_4(CO)_{39}]^{4-}$ and $[HNi_{31}P_4(CO)_{39}]^{5-}$.

	Ni-Ni	Ni-P
$[Ni_{11}P(CO)_{18}]^{3-}$	2.3820(19)-3.138(2) Average 2.627(10)	2.314(3)-2.440(3) Å Average 2.351(9)
$[H_2Ni_{31}P_4(CO)_{39}]^{4-}$ [a]	2.381(3)-3.237(8) Average 2.598(16)	2.155(3)-3.094(3) Average 2.343(15)
$[HNi_{31}P_4(CO)_{39}]^{5-}$ [b]	2.399(4)-3.315(5) Average 2.65(4)	2.147(7)-3.157(7) Average 2.35(4)
$[H_2Ni_{31}P_4(CO)_{39}]^{4-}$ /$[HNi_{31}P_4(CO)_{39}]^{5-}$ [c]	2.4160(10)-3.300(2) Average 2.662(10)	2.154(2)-3.176(2) Average 2.364(8)

[a] Some longer Ni-Ni and Ni-P distances have been included for geometrical reasons, even if they are rather long to be classified as proper bonds.
[b] as found in $[NEt_4]_4[H_2Ni_{31}P_4(CO)_{39}]\cdot 2CH_3COCH_3$.
[c] as found in $[NEt_4]_6[HNi_{31}P_4(CO)_{39}][Cl]\cdot 2CH_3CN$.
[d] as found in $[NEt_4]_6[H_2Ni_{31}P_4(CO)_{39}]_{0.46}[HNi_{31}P_4(CO)_{39}]_{0.54}[NiCl_4]_{0.46}[BF_4]_{0.54}\cdot 2CH_3COCH_3$.

Encapsulation of a P-atom within a M_{10}-sphenocorona cage is unprecedented in molecular cluster chemistry. Previous examples of fully interstitial monophosphide carbonyl clusters suggested the preference for trigonal prismatic or square-antiprismatic cages, as in the case of Os, Ru, Rh and Co clusters.[45-53] Because of the larger radius, Os clusters adopted trigonal prismatic structures, whereas smaller metals preferred a larger square-antiprismatic cage. Moreover, it must be remarked that the $Ni_{12}P_5$ phase contains two inequivalent P-atoms, and one of them is encapsulated within a Ni_{10}-sphenocorona.[9-13]

The range of 25 Ni-Ni bonding contacts is broad [2.3820(19)-3.138(2) Å, average 2.627(10) Å], whereas the 10 Ni-P bonds are comprised in a rather narrow range [2.314(3)-2.440(3) Å, average 2.351(9) Å], and compare quite well with those found for the $Ni_{10}P$ sphenocorona cage of $Ni_{12}P_5$ [2.229-2.596 Å, average 2.390 Å].[9-13] The molecule is completed by 18 CO ligands, 8 terminal and 10 edge-bridging.

The cluster possesses 154 cluster valence electrons (CVE), which correspond to 6n+11 cluster molecular orbitals (CMO). Based on the capping principle,[57] the Ni(CO) fragment not bonded to P can be excluded from the electron count, resulting in a ten vertices clusters with 142 CVE and again 6n+11 CMO. The same electron count has been found in the bicapped square-antiprismatic clusters $[Rh_{10}P(CO)_{22}]^-$,[48,49] $[Rh_{10}As(CO)_{22}]^-$,[58] and $[Rh_{10}S(CO)_{22}]^{2-}$,[59] even if their structures differ from $[Ni_{11}P(CO)_{18}]^{3-}$.

2.2 Synthesis and molecular structure of $[H_{6-n}Ni_{31}P_4(CO)_{39}]^{n-}$ (n = 4 and 5).

$[Ni_{11}P(CO)_{18}]^{3-}$ was readily oxidized by further addition of PCl_3 yielding $[HNi_{31}P_4(CO)_{39}]^{5-}$ in agreement with

$$3[Ni_{11}P(CO)_{18}]^{3-} + PCl_3 + H_2O \rightarrow [HNi_{31}P_4(CO)_{39}]^{5-} + 3Cl^- + 2Ni(CO)_4 + CO + OH^- \quad (2)$$

$[HNi_{31}P_4(CO)_{39}]^{5-}$ can be obtained also by oxidation of $[Ni_{11}P(CO)_{18}]^{3-}$ with $[C_7H_7][BF_4]$ or, more conveniently by reacting $[NEt_4]_2[Ni_6(CO)_{12}]$ in thf with 0.8-0.9 equivalents of PCl_3, in accord to reaction 3. The presence of moisture cannot be completely excluded, and this is the reason why H_2O is present in both equations 2 and 3 as proton source.

$$6[Ni_6(CO)_{12}]^{2-} + 4PCl_3 + H_2O \rightarrow [HNi_{31}P_4(CO)_{39}]^{5-} + 12Cl^- + 3Ni^{2+} + 2Ni(CO)_4 + 25CO + OH^- \quad (3)$$

At the end of the reaction, $Ni(CO)_4$ (as detected by IR) was removed under reduced pressure, the Ni(II) salts washed with water, traces of $[Ni_{11}P(CO)_{18}]^{3-}$ extracted in acetone and, eventually, $[HNi_{31}P_4(CO)_{39}]^{5-}$ was extracted in CH_3CN. Crystals of $[NEt_4]_6[HNi_{31}P_4(CO)_{39}][Cl]\cdot 2CH_3CN$ suitable for X-ray crystallography were obtained by slow diffusion of n-hexane and diisopropyl ether into the CH_3CN solution. These crystals display ν_{CO} bands at 2009(s), 1873(m) cm^{-1} in CH_3CN solution. $[HNi_{31}P_4(CO)_{39}]^{5-}$ is readily protonated to $[H_2Ni_{31}P_4(CO)_{39}]^{4-}$ after addition of $HBF_4\cdot Et_2O$ to the CH_3CN solution, as indicated by the shift of the ν_{CO} bands to 2022(s), 1876(m) and 1818(w) cm^{-1}. The tetra-anion is soluble in acetone, and crystals of $[NEt_4]_4[H_2Ni_{31}P_4(CO)_{39}]\cdot 2CH_3COCH_3$ suitable for X-ray diffraction were obtained by slow diffusion of n-hexane into the acetone solution.

Similarly, the penta-anion was deprotonated to the $[Ni_{31}P_4(CO)_{39}]^{6-}$ hexa-anion after reaction with CH_3ONa in CH_3CN, as confirmed by the shift to lower frequencies of the ν_{CO} bands at 1997(s), 1859(m) cm^{-1} (Scheme 1). In turn, the purported fully deprotonated $[Ni_{31}P_4(CO)_{39}]^{6-}$ hexa-anion was reduced by Na/naphthalene in dmf affording the $[Ni_{31}P_4(CO)_{39}]^{7-}$ epta-anion (ν_{CO} at 1976(s), 1839(m) cm^{-1} in dmf).

Scheme 1. Reactivity of $[HNi_{31}P_4(CO)_{39}]^{5-}$.

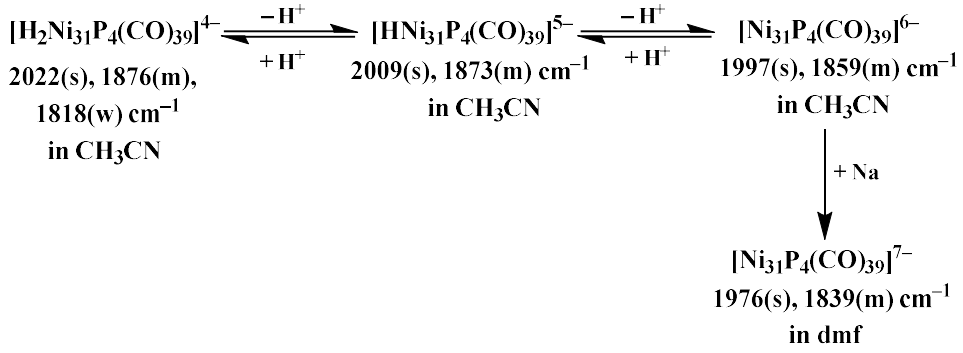

Formulation of the $[H_{6-n}Ni_{31}P_4(CO)_{39}]^{n-}$ species as polyhydrides was indirectly inferred from electrochemical and spectroelectrochemical studies (see Section 2.3) as well as their acid-base and redox chemical reactions summarized in Scheme 1. Indeed, as previously discussed for other large molecular metal carbonyl clusters,[14,23,32,60,61] all attempts to directly confirm their polyhydride nature by ^{1}H NMR spectroscopy failed under any adopted experimental condition (solution and solid state experiments; VT experiments; different spectrometer frequencies; ^{1}H/^{2}D replacement and ^{2}D NMR spectroscopy in solution). Up to now, the largest molecular metal carbonyl clusters for which there is direct evidence (by ^{1}H NMR spectroscopy) of the presence of hydride ligands as well as of the occurrence of protonation-deprotonation reactions are $[H_{4-n}Ni_{22}(C_2)_4(CO)_{28}(CdBr)_2]^{n-}$ (n = 2–4) and $[H_{8-n}Rh_{22}(CO)_{35}]^{n-}$ (n = 3-7).[14,23,32,60,61] It must be remarked that the former Ni-clusters display very broad and temperature dependent ^{1}H NMR spectra, whereas these phenomena are more limited in the case of the Rh_{22}-clusters. Nonetheless, all higher nuclearities molecular metal carbonyl clusters are ^{1}H NMR silent, independent of the nature of the metal atoms. In addition, the differently charged $[H_{4-n}Ni_{22}(C_2)_4(CO)_{28}(CdBr)_2]^{n-}$ (n = 2–4) and $[H_{8-n}Rh_{22}(CO)_{35}]^{n-}$ (n = 3-7) hydride clusters displayed different voltammetric profiles as a further proof of their polyhydride nature. Indeed, electrochemistry seems to be the best technique in order to prove (at least indirectly) the hydrido nature of larger molecular metal carbonyl clusters, when ^{1}H NMR spectroscopy fails. Thus, if two isostructural clusters differing only by the charge display different electrochemical properties, then they ought to be hydrides. Conversely, if they show identical electrochemical properties, then they are the same chemical species but more or less oxidised.[14,23,32,60,61]

In the present case, the isostructural (see below) $[HNi_{31}P_4(CO)_{39}]^{5-}$ and $[H_2Ni_{31}P_4(CO)_{39}]^{4-}$ anions can be easily inter-converted by means of acid-base reactions. As they display different electrochemical and spectroelectrochemical properties (see Section 2.3), they should be two different chemical species with a different number of hydride atoms. These, indeed, cannot be detected by X-ray crystallography in such large clusters, and may explain the different charges observed for the two clusters. Moreover, it is well known that hydrides in metal carbonyls are acidic and can be added/removed via acid-base reactions. The total number of hydrides in each species has been indirectly inferred from the number of observed protonation/deprotonation reactions. Thus, the $[H_2Ni_{31}P_4(CO)_{39}]^{4-}$ tetra-anion can be transformed into the $[HNi_{31}P_4(CO)_{39}]^{5-}$ penta-anion by addition of a base. In turn, the penta-anion is converted into the $[Ni_{31}P_4(CO)_{39}]^{6-}$ hexa-anion by further increasing the amount and/or strength of the base. Both these reactions can be reversed by addition of stoichiometric amounts of a strong acid such as $HBF_4{\cdot}Et_2O$. Conversely, the $[Ni_{31}P_4(CO)_{39}]^{7-}$ epta-anion can be obtained from the hexa-anion only by reaction with a strong

reducing agent such as Na/naphthalene. Thus, we can speculate that the $[Ni_{31}P_4(CO)_{39}]^{6-}$ hexa-anion is the fully deprotonated cluster, even if we cannot completely rule out the presence of further hydride ligands. Overall, all the data available, at least indirectly, support the assumption that these large nanoclusters are polyhydride and the differently charged species contain a different number of hydride ligands. The total number of such ligands in each species must be taken as a mere hypothesis.

The molecular structure of $[H_{6-n}Ni_{31}P_4(CO)_{39}]^{n-}$ (n = 4, 5) was determined as its $[NEt_4]_4[H_2Ni_{31}P_4(CO)_{39}]\cdot 2CH_3COCH_3$, $[NEt_4]_6[HNi_{31}P_4(CO)_{39}][Cl]\cdot 2CH_3CN$ and $[NEt_4]_6[H_2Ni_{31}P_4(CO)_{39}]_{0.46}[HNi_{31}P_4(CO)_{39}]_{0.54}[NiCl_4]_{0.46}[BF_4]_{0.54}\cdot 2CH_3COCH_3$ salts (Figure 2 and Table 1). The presence of Cl^- and $[NiCl_4]^{2-}$ anions within the crystals is due to the fact that they are byproducts in the synthesis of these clusters (see eq 3), which cannot be completely washed out during the workup. Similarly, the $[BF_4]^-$ anion in the crystals of $[NEt_4]_6[H_2Ni_{31}P_4(CO)_{39}]_{0.46}[HNi_{31}P_4(CO)_{39}]_{0.54}[NiCl_4]_{0.46}[BF_4]_{0.54}\cdot 2CH_3COCH_3$ is due to the use of $HBF_4{\cdot}Et_2O$ as proton source. The molecular structure and bonding parameters of the cluster are the same in all the three salts, even if the anionic charges are different. This observation is in agreement with the assumption that the tetra- and penta-anion differ only because of a different number of hydride ligands. The $Ni_{31}P_4$ cage (Figure 3) can be viewed as composed of two distorted Ni_9P mono-capped square anti-prisms and two distorted $Ni_{10}P$ bi-capped square antiprisms (Figure 4) fused together resulting in a $Ni_{29}P_4$ framework. This is capped by two additional Ni-atoms which are not bonded to any phosphorous (in yellow in Figure 3). The cluster contains two fully interstitial Ni-atoms (in blue in Figure 3), 100 Ni-Ni bonding contacts and 38 Ni-P interactions. The two interstitial Ni atoms are bonded together [$Ni_{interstitial}$-$Ni_{interstitial}$ 2.514(2), 2.533(4) and 2.5392(18) Å for the three salts, respectively] and display 11 Ni-Ni and 3 Ni-P contacts. The cluster is completed by 39 CO ligands, of which there are 14 terminal, 23 edge bridging and 2 face bridging.

Three Ni-P phases containing isolated phosphides are known: Ni_3P, Ni_2P and $Ni_{12}P_5$.[9-13] The P-atom is encapsulated within a distorted mono-capped square anti-prismatic cage in Ni_3P and a tri-capped trigonal prismatic cage in Ni_2P. Conversely, in $Ni_{12}P_5$ one P-atom is contained within a sphenocorona cage and the other within a cubic cage.

Previous to this work, the only molecular carbonyl clusters containing more than one P-atom were the $Co_2P_2(CO)_{19}$, $Co_{10}P_2(CO)_{24}$ and $[HCo_{10}P_2(CO)_{23}]^{2-}$,[51,52] di-phosphides all presenting the P-atoms in semi-interstitial positions. Thus, the $[H_{6-n}Ni_{31}P_4(CO)_{39}]^{n-}$ (n = 4 and 5) clusters represent the first cases of structurally characterized molecular fully interstitial poly phosphide clusters.

A nuclearity of 31 is rather rare among metal carbonyl clusters, and only four examples have been reported in the literature: $[Au_{21}Fe_{10}(CO)_{40}]^{5-}$,[62] $[H_2Ni_{29}Cu_2C_4(CO)_{34}(MeCN)_2]^{2-}$,

$[H_2Ni_{29}Cu_2C_4(CO)_{32}(MeCN)_4]^{2-}$,[23b] and $[Ni_{31}Sb_4(CO)_{40}]^{6-}$.[37] The latter is closely related to $[H_{6-n}Ni_{31}P_4(CO)_{39}]^{n-}$ (n = 4 and 5), since it contains four pnictogen atoms, but these are semi-interstitial and not fully interstitial.

The $[H_{6-n}Ni_{31}P_4(CO)_{39}]^{n-}$ (n = 4 and 5) clusters are electron rich, displaying 414 CVE (6n+21 CMO). $[Ni_{31}Sb_4(CO)_{40}]^{6-}$ is even electron richer, possessing 416 CVE (6n+22). Such rich electron counts are usual for large nickel carbonyl clusters containing several interstitial heteroatoms, as usually found in polycarbide nickel carbonyls.[30-34]

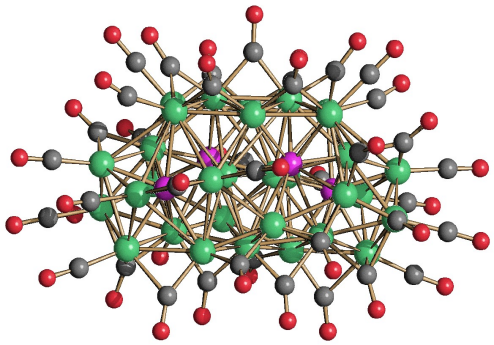

Figure 2. Molecular structure of $[H_{6-n}Ni_{31}P_4(CO)_{39}]^{n-}$ (n = 4 and 5) (Ni, green; P, purple; C, grey; O, red).

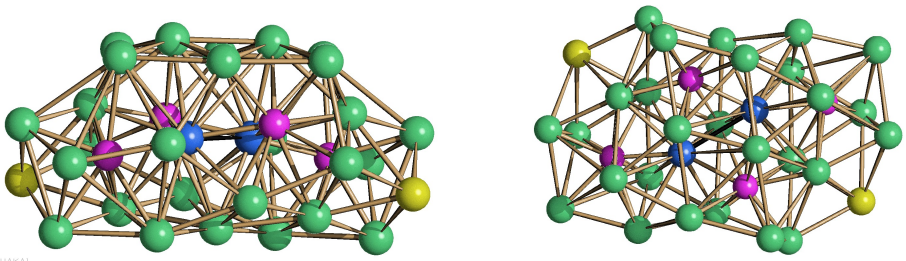

Figure 3. Two different views of the $Ni_{31}P_4$ core of $[H_{6-n}Ni_{31}P_4(CO)_{39}]^{n-}$ (n = 4, 5) (Ni, green; fully interstitial Ni, blue; Ni not bonded to P, yellow; P, purple).

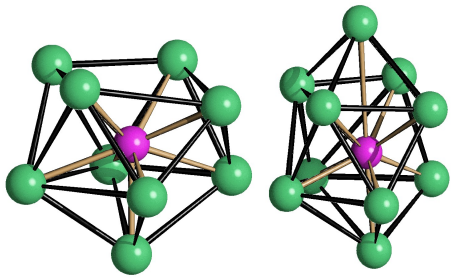

(a) (b)

Figure 4. (a) The Ni_9P mono-capped square anti-prism and (b) the $Ni_{10}P$ bicapped square anti-prism present in $[H_{6-n}Ni_{31}P_4(CO)_{39}]^{n-}$ (n = 4 and 5) (Ni, green; P, purple).

2.3 Electrochemical and spectroelectrochemical studies of $[Ni_{11}P(CO)_{18}]^{3-}$, $[HNi_{31}P_4(CO)_{39}]^{5-}$ and $[H_2Ni_{31}P_4(CO)_{39}]^{4-}$.

The redox chemistries of $[Ni_{11}P(CO)_{18}]^{3-}$ and $[H_{6-n}Ni_{31}P_4(CO)_{39}]^{n-}$ (n = 4 and 5) in CH_3CN solution were studied by cyclic voltammetry and *in situ* infrared spectoelectrochemistry in an optically transparent thin-layer electrochemical (OTTLE) cell. The potential of the working electrode (WE) was swept between the selected potentials at the scan rate of 0.5 mV s^{-1} and a sequence of IR spectra in the CO stretching region was collected at constant time intervals. On the basis of the profile of the *i/E* curve recorded during the slow potential scan, the IR spectra were separated and assigned to the different products formed after each electron exchange process. In this way, we were able to select the IR spectra (in the ν_{CO} region) of the different redox states of the clusters.

The voltammetric profile exhibited by $[Ni_{11}P(CO)_{18}]^{3-}$ shows several ill-defined processes. Because of their low current density, the experimental determination of the electrochemical and chemical reversibility of these processes, as well as the determination of the number of electrons involved in each redox step, is rather difficult. The strong peak at -0.33 V (*vs* Ag/AgCl), irreversible also in the time scale of the cyclic voltammetry, indicates that the cluster can be oxidized in a redox step that presumably involves more than one electron. Two or three quasi-reversible or irreversible reduction processes were hardly detectable between -0.8 and -2.2 V.

More information regarding the redox transformations of $[Ni_{11}P(CO)_{18}]^{3-}$ in $CH_3CN/[N^nBu_4][PF_6]$ have been obtained by IR spectroelectrochemistry. When the potential of the working electrode (WE) is swept between -0.8 and -1.6 V, the ν_{CO} bands of the starting cluster (1980 and 1845 cm^{-1}) were downshifted at 1960 and 1835 cm^{-1} suggesting the formation of the $[Ni_{11}P(CO)_{18}]^{4-}$ tetra-anion. The IR spectrum of $[Ni_{11}P(CO)_{18}]^{3-}$ was restored in the reverse potential scan from -1.6 to -0.8 V pointing out the stability of the electrogenerated reduced species. Further changes of the infrared spectra were observed lowering the applied potential up to -2.3 V. In particular, moving the potential from -1.6 and -1.9 V, the terminal ν_{CO} band shifted at 1952 cm^{-1}, and in the bridging ν_{CO} region, three bands appeared at 1836, 1815 and 1798 cm^{-1}, in a completely reversible transformation (Figure 5b). The low current intensity associated with slight changes of the IR spectrum suggested the presence of an impurity.

On lowering the WE potential from -1.9 to -2.3 V, new ν_{CO} bands appear at 1945, 1928, 1899, 1873, 1816, 1790, 1770 and 1713 cm^{-1} (Figure 5c) suggesting major structural changes and incipient decomposition. These phenomena were also indicated by the reduced intensity of the ν_{CO} bands of $[Ni_{11}P(CO)_{18}]^{3-}$ restored in the backward potential scan from -2.3 V to -0.8 V.

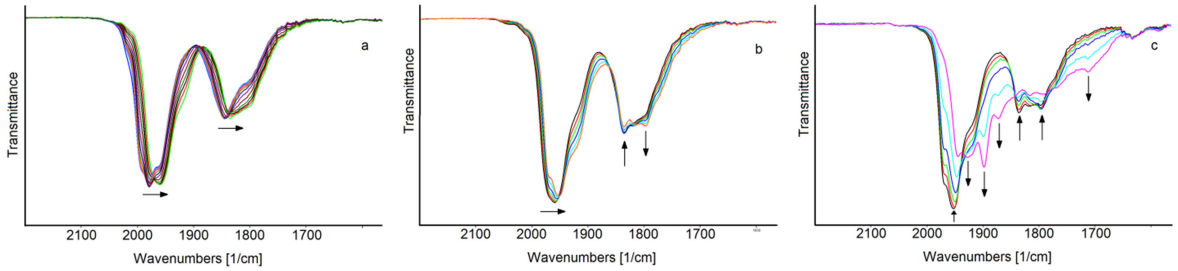

Figure 5. IR spectral changes of a CH_3CN solution of $[Ni_{11}P(CO)_{18}]^{3-}$ recorded in an OTTLE cell during the progressive reduction of the potential a) from -0.8 to -1.6 V; b) from -1.6 to -1.9 V; c) from -1.9 to -2.3 V. $[N^nBu_4][PF_6]$ (0.1 mol dm^{-3}) as the supporting electrolyte. The absorptions of the solvent and the supporting electrolyte have been subtracted.

Concerning the oxidation process of $[Ni_{11}P(CO)_{18}]^{3-}$, when the electrode potential is swept from -0.6 to +0.1 V, a gradual and continuous shift of the ν_{CO} bands to higher wavenumbers (2074(w), 2024(vs), 1872(m) cm^{-1}) was observed. Moreover, the shape and intensity of the ν_{CO} bands attributable to bridging carbonyls were considerably modified. In the relative current-potential profile, a constant increase of the oxidation current was observed. This made impossible to separate the IR spectra and assign them to different oxidation process. In the reverse reduction backs can, the opposite trend was observed, but the IR spectrum of $[Ni_{11}P(CO)_{18}]^{3-}$ was obtained only at -1.7 V (See Supporting Information Figure S.1). These results, suggest that the oxidation is presumably a process that involves more than one electron and that the electrogenerated oxidized species decomposes to give a new cluster as well as $Ni(CO)_4$, as shown by its typical ν_{CO} band at 2042 cm^{-1} in the final spectrum. This new (and yet not identified) cluster may be transformed back into $[Ni_{11}P(CO)_{18}]^{3-}$ by lowering the potential to -1.7 V.

These results indicate that $[Ni_{11}P(CO)_{18}]^{3-}$ possesses an intermediate redox behavior between that of smaller carbonyl clusters, which display a precise electron count, and that of higher nuclearity metal carbonyl clusters, which undergo several reversible redox processes. Accordingly, only one chemically reversible reduction process, presumably monoelectronic, was detected in the case of $[Ni_{11}P(CO)_{18}]^{3-}$. Conversely, at more positive potentials, an oxidative redox condensation process presumably converts this smaller cluster into larger ones. Unfortunately, the *in situ* spectroelectrochemical investigation of the process does not allow the detection of the labile oxidized intermediates.

The redox behavior of the larger penta-anion $[HNi_{31}P_4(CO)_{39}]^{5-}$ was preliminarily investigated by cyclic voltammetry between -0.3 and -2.3 V at a Pt electrode in $CH_3CN/[N^nBu_4][PF_6]$ solution. Under these conditions, several processes with apparent features of

reversibility were observed: two oxidations at -0.78 and -0.49 V and three reductions at -1.15, -1.46 and -2.06 V. Unfortunately, the solubility of this large nanocluster was rather limited in the presence of the supporting electrolyte in large excess. As a result, the current densities measured in the cyclic voltammetries were very low, and the processes observed were complicated, in some cases, by adsorption phenomena. Therefore, the electrochemical patterns never had a high resolution, and their complete characterization by cyclic voltammetry was almost impossible Thus, the rich reversible redox chemistry of $[HNi_{31}P_4(CO)_{39}]^{5-}$ was further ascertained through *in situ* spectroelectrochemical FTIR, which resulted in a satisfactory description of the different redox states of this cluster. In particular, the ν_{CO} bands of the cluster moved toward higher (or lower) wavenumbers upon each anodic (or cathodic)step, and the original spectra were restored upon inversion of the potential. Detail of the different anodic and cathodic processes observed are given below.

When the potential of the working electrode was swept between -1.0 and -0.6 V (Figure 6), the chemically reversible oxidation of the cluster is accompanied by the shift of the ν_{CO} bands from 2009 and 1873 cm^{-1}, to 2022 and 1882 cm^{-1}. A progressive shift at higher wavenumbers (2040 and 1892 cm^{-1}) was, then, observed on further increasing the applied potential up to -0.3 V. At the same time, during the progressive oxidation of the cluster, the intensity of the ν_{CO} band of the terminal carbonyls increased compared to the bridging ones. This is in agreement with the fact that, by decreasing the negative charge of a carbonyl cluster, terminal CO ligands are more favored than bridging ones.[63] This slight change of the stereochemistry of the CO ligands makes the second oxidation process electrochemically quasi-reversible. The stability of both the oxidized species was verified through a backward potential scan from -0.3 V to -1.0 V, that restored the IR spectrum of $[HNi_{31}P_4(CO)_{39}]^{5-}$.

A further increase of the potential of the working electrode from -0.3 to -0.1 V leads to the irreversible decomposition of the cluster and formation of $Ni(CO)_4$ (ν_{CO} 2042 cm^{-1}) as the only detectable carbonyl species.

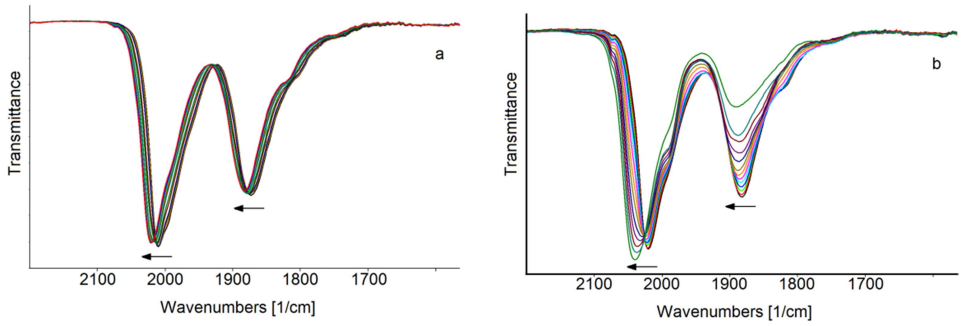

Figure 6. IR spectral changes of a CH_3CN solution of $[HNi_{31}P_4(CO)_{39}]^{5-}$ recorded in an OTTLE cell during the progressive increase of the potential a) from –1.0 to -0.6 V; b) from -0.6 to -0.3 V. $[N^nBu_4][PF_6]$ (0.1 mol dm^{-3}) as the supporting electrolyte. The absorptions of the solvent and the supporting electrolyte have been subtracted.

When the potential of the working electrode was swept between -1.0 and -2.6 V, six reduction processes have been identified from the analysis of the complete sequence of the recorded IR spectra. In particular, four reduction processes were observed in the profile of the *i/E* curve obtained during the slow cathodic scan of the potential from -1.0 to -2.2 V. Two further reductions of the cluster at lower potentials were hidden by the solvent discharge in the *i/E* curve, but their occurrence is clearly demonstrated by the analysis of the IR spectra recorded during the spectroelectrochemical experiments (see Supporting Information Figure S.2).

All the reduction steps are completely chemically reversible and the potential can be cycled between -1.0 and -2.6 V without decomposition of the electrogenerated species. Indeed, the IR spectrum of the starting cluster $[HNi_{31}P_4(CO)_{39}]^{5-}$ was restored when the working electrode potential was returned to the initial value (-1.0 V).

As already found for platinum high nuclearity clusters,[23c] well defined isosbestic points are not always observable for each process. Carbonyl absorptions often shifted to higher or lower frequencies, depending on the sweep potential, without a well-defined isosbestic point. However, both the terminal and bridging ν_{CO} bands retained their shape and relative intensity on changing the cluster charge, except during the second oxidation process.

All these observations, together with the complete chemical reversibility of the eight redox processes observed between -0.3 and -2.6 V, pointed out that the structure of $[HNi_{31}P_4(CO)_{39}]^{5-}$ is stable with a variable number of electrons. Only minor structural changes occur on the time scale of the spectroelectrochemical experiments, except in the case of the most anodic process. Thus, the modifications of the shape and intensity of the IR spectrum of the most oxidized cluster, compared to the other species, suggested the occurrence of important structural changes especially regarding the stereochemistry of the CO ligands.

By comparing of the stretching frequencies of terminal CO ligands belonging to the reversible redox states of the cluster (Table 2), we observed for all the processes a near-uniform shift of 14 cm^{-1}. A similar trend was previously observed in the case of redox active metal carbonyl clusters with similar nuclearities[14,23,25,29,54,55] and was indicative of one-electron transfers. Therefore, the electron rich cluster $[HNi_{31}P_4(CO)_{39}]^{5-}$, like other high nuclearity ones, can be

defined multivalent as it is able to reversibly release two electrons and to accept up to six electrons.[55b]

Table 2. Infrared stretching frequencies (cm^{-1}) of terminal (ν^t_{CO}) and bridging (ν^b_{CO}) carbonyl groups for $[HNi_{31}P_4(CO)_{39}]^{n-}$ in CH_3CN as a function of the cluster charge *n* and of the potential *E*.

Cluster charge n	ν^t_{CO}	ν^b_{CO}	*E*
3	2040	1892	-0.30 V
4	2022	1882	-0.60 V
5	2009	1873	-1.0 V
6	1995	1864	-1.41 V
7	1982	1852	-1.68V
8	1965	1841	-1.92 V
9	1951	1825	-2.19 V
10	1939	1809	-2.34V
11	1928	1799	-2.55 V

A different number of hydride ligands in the isostructural $[HNi_{31}P_4(CO)_{39}]^{5-}$ and $[H_2Ni_{31}P_4(CO)_{39}]^{4-}$ anions was inferred by the comparison of their electrochemical and spectroelectrochemical properties. Despite the poor cyclic voltammetric response obtained with these large clusters, the voltammetric profile exhibited by $[H_2Ni_{31}P_4(CO)_{39}]^{4-}$ at a Pt electrode in $CH_3CN/[N^nBu_4][PF_6]$ solution, between -0.1 and -2.4 V, is quite different from that of the isostructural $[HNi_{31}P_4(CO)_{39}]^{5-}$ (See Supporting Information Figure S.3). In particular, $[H_2Ni_{31}P_4(CO)_{39}]^{4-}$ showed only three reduction processes (at -0.55, -0.78 and -1.7 V), with some features of chemical and electrochemical reversibility (see spectroelectrochemical experiments), and one irreversible oxidation, at potentials higher than -0.4 V. Conversely, $[HNi_{31}P_4(CO)_{39}]^{5-}$ displayed two oxidations and six reductions (see above). As discussed in the case of $[HNi_{31}P_4(CO)_{39}]^{5-}$, a better insight on the redox behavior of $[H_2Ni_{31}P_4(CO)_{39}]^{4-}$ was obtained through FTIR spectroelectrochemical experiments.

The $[H_2Ni_{31}P_4(CO)_{39}]^{4-}$ cluster displayed ν_{CO} bands at 2022(s), 1876(m) and 1818(w) cm^{-1} in $CH_3CN/[N^nBu_4][PF_6]$ solution. These bands are shifted at lower wavenumbers during the slow decrease of the working electrode potential from -0.3 to -2.1 V in an OTTLE cell (see Supporting Information Figure S.4). The original spectra were restored in the reverse potential back-scan, revealing the presence of three chemically reversible reduction processes (Table 3). At lower potentials a fast decomposition reaction was observed, as inferred from the appearance in the IR spectrum of new absorptions, that did not regenerate the original spectrum on increasing the potential. Similarly, when the working electrode potential was increased above -0.3 V, the irreversible decomposition of $[H_2Ni_{31}P_4(CO)_{39}]^{4-}$ was observed.

Table 3. Infrared stretching frequencies (cm^{-1}) of terminal (ν^t_{CO}) and bridging (ν^b_{CO}) carbonyl groups for $[H_2Ni_{31}P_4(CO)_{39}]^{n-}$ in CH_3CN as a function of the cluster charge *n* and of the potential *E*.

Cluster charge n	ν^t_{CO}	ν^b_{CO}	*E*
4	2022	1876, 1818	-0.40 V
5	2011	1864, 1806	-0.70 V
6	1994	1847, 1780	-1.15 V
7	1980	1841	-1.75 V

By comparison of the data reported in Tables 2 and 3, it is evident that when the $[H_xNi_{31}P_4(CO)_{39}]^{n-}$ (x = 1, 2; n = 4, 5, 6, 7) clusters have the same charge have they possess very similar IR spectra in the ν_{CO} region. Nonetheless, if we overlay two by two the spectra of the $[H_2Ni_{31}P_4(CO)_{39}]^{n-}$and $[HNi_{31}P_4(CO)_{39}]^{n-}$ clusters with the same charge *n* (Figure 7), we can notice some small but yet significant differences, particularly in the region of the μ-CO stretching absorptions. This, in turn, supports the assumption that the two clusters are different. More importantly, the fact that during the spectroelectrochemical experiments nine different redox states have been identified in the case of $[HNi_{31}P_4(CO)_{39}]^{5-}$, whereas there is evidence of only four redox states of $[H_2Ni_{31}P_4(CO)_{39}]^{4-}$ (Table 2 and 3), which clearly support the conclusion that the two clusters are different molecular species and not the same molecular cluster more or less oxidizes (or reduced). Thus, since the tetra- and penta-anions are isostructural and the only atoms which cannot be observed by X-ray crystallography in such large metal nanoclusters are hydrogen atoms, it is reasonable to conclude that they contain a different number of hydride ligands.

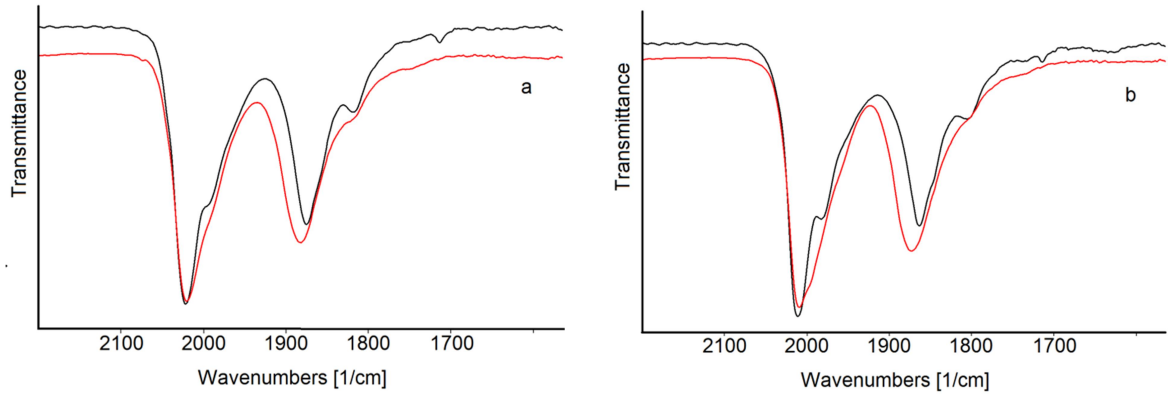

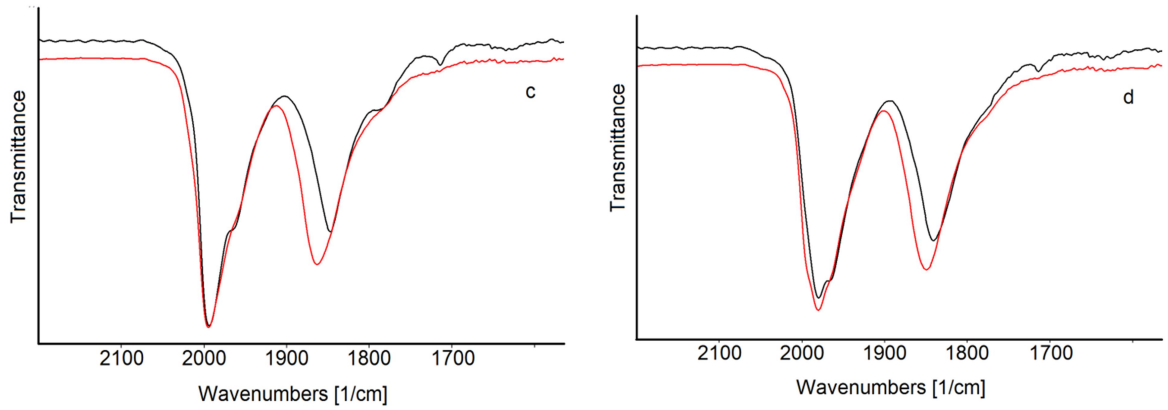

Figure 7. Comparison between the IR spectra of a CH_3CN solution of $[H_2Ni_{31}P_4(CO)_{39}]^{n-}$ (black) and $[HNi_{31}P_4(CO)_{39}]^{n-}$ (red) recorded in an OTTLE cell at different potentials of the working electrode; a) n = 4; b) n = 5; c) n = 6; d) n = 7. $[N^nBu_4][PF_6]$ (0.1 mol dm^{-3}) as the supporting electrolyte. The absorptions of the solvent and the supporting electrolyte have been subtracted.

3. Conclusions

In this paper we have reported the first examples of Ni-carbonyl clusters containing fully interstitial P-atoms, *i.e.*, $[Ni_{11}P(CO)_{18}]^{3-}$ and $[H_{6-n}Ni_{31}P_4(CO)_{39}]^{n-}$ (n = 4,5). These add to the family of Ni clusters containing fully interstitial or semi-interstitial hetero-atoms, such as C, Ga, Ge, Sn, Sb, Bi.[25,29] The $[H_{6-n}Ni_{31}P_4(CO)_{39}]^{n-}$ (n = 4 and 5) clusters represent also the first cases of structurally characterized molecular fully interstitial poly-phosphide clusters.

The data herein reported confirm the ability of interstitial heteroatoms to increase the stability of metal carbonyl clusters, favoring the formation of higher nuclearity species.[14,25,29,30-39] As a further consequence of this enhanced stability, large molecular metal carbonyl clusters containing interstitial heteroatoms are often multivalent and may display several reversible redox processes. This point is demonstrated by comparing the rich redox behavior of $[H_{6-n}Ni_{31}P_4(CO)_{39}]^{n-}$ (n = 4,5) with the fact that, in the case of $[Ni_{11}P(CO)_{18}]^{3-}$, spectroelectrochemical studies demonstrate only the reversible formation of the tetra-anion $[Ni_{11}P(CO)_{18}]^{4-}$. This points out the incipient metallization of the metal core of a cluster as a function of its nuclearity.[14,29]

The main drawback of this work is the fact that often higher nuclearity metal carbonyl clusters are also polyhydrides.[14,23,32,60,61] Thus, their charges can be changed by means of redox reactions, *via* addition/removal of electrons, as well as acid/base reactions, *via* addition/removal of H^+. Thus, their total characterization is a challenge for the actual molecular analytical techniques, and this finds a parallel in the field of atomically precise colloidal metal nanoclusters and nanoparticles.[14,15] At the moment, we have been able only to indirectly prove the polyhydrido nature of these molecular nanoclusters on the basis of their different electrochemical and more

importantly spectroelectrochemical properties. The fact that the isostructural $[HNi_{31}P_4(CO)_{39}]^{5-}$ and $[H_2Ni_{31}P_4(CO)_{39}]^{4-}$ clusters display different redox properties points out that they are different molecular species. It is reasonable to assume that they differ only because of a different number of hydride ligands, since hydrogen atoms are not detected by X-ray crystallography in such large metal nanoclusters. The total number of hydride in each species has been based solely on the number of the observed protonation/deprotonation reactions and, therefore, must be taken as a mere hypothesis.

Finally, the molecular clusters herein reported are structurally related to extended Ni-P phases, *i.e.*, Ni_3P, Ni_5P_2, $Ni_{12}P_5$, Ni_2P, Ni_5P_4, NiP, NiP_2 and NiP_3.[9-13] Thus, they may be viewed as models and precursors of ultra-small Ni-P nanoparticles. Work is now underway in order to prepare larger molecular Ni-P carbonyl nanoclusters and use them for the preparation of Ni-phosphide nanoparticles.

4. Experimental

4.1 General procedures.

All reactions and sample manipulations were carried out using standard Schlenk techniques under nitrogen and in dried solvents. All the reagents were commercial products (Aldrich) of the highest purity available and used as received, except $[NEt_4]_2[Ni_6(CO)_{12}]$ which has been prepared according to the literature.[64] Analysis of Ni were performed by atomic absorption on a Pye-Unicam instrument. Analyses of C, H and N were obtained with a Thermo Quest Flash EA 1112NC instrument. IR spectra were recorded on a Perkin Elmer Spectrum One interferometer in CaF_2 cells. Structure drawings have been performed with SCHAKAL99.[65]

4.2 Synthesis of $[NEt_4]_3[Ni_{11}P(CO)_{18}]$

A solution of PCl_3 (0.148 g, 1.08 mmol) in thf (60 mL) was added to a solution of $[NEt_4]_2[Ni_6(CO)_{12}]$ (1.95 g, 2.06 mmol) in thf (20 mL) over a period of 4 h. The resulting mixture was stirred at room temperature for 1 h and, then, the solvent removed *in vacuo*. The residue was washed with H_2O (3×20 mL), thf (3×20 mL), and extracted with acetone (20 mL). Crystals of $[NEt_4]_3[Ni_{11}P(CO)_{18}]$ suitable for X-ray analyses were obtained by layering n-hexane (40 mL) on the acetone solution (yield 0.36 g, 20 % based on Ni).

$C_{42}H_{60}N_3Ni_{11}O_{18}P$ (1571.71): calcd. C 32.10, H 3.85, N 2.67, Ni 41.08; found: C 31.88, H 3.77, N 2.92, Ni 40.91. IR (CH_3CN, 293 K) ν_{CO}: 1980(s), 1845(m) cm^{-1}.

4.3 Synthesis of $[NEt_4]_6[HNi_{31}P_4(CO)_{39}][Cl]\cdot 2CH_3CN$

A solution of PCl_3 (0.259 g, 1.89 mmol) in thf (100 mL) was added to a solution of $[NEt_4]_2[Ni_6(CO)_{12}]$ (1.95 g, 2.06 mmol) in thf (20 mL) over a period of 6 h. The resulting mixture was stirred at room temperature for 1 h and, then, the solvent removed *in vacuo*. The residue was washed with H_2O (3×20 mL), thf (3×20 mL), and extracted with CH_3CN (20 mL). Crystals of $[NEt_4]_6[HNi_{31}P_4(CO)_{39}][Cl]\cdot 2CH_3CN$ suitable for X-ray analyses were obtained by layering n-hexane (4 mL) and di-iso-propyl-ether (40 mL) on the CH_3CN solution (yield 0.81 g, 52 % based on Ni).

$C_{91}H_{123}ClN_8Ni_{31}O_{39}P_4$ (3932.31): calcd. C 27.80, H 3.15, N 2.85, Ni 46.28; found: C 27.65, H 3.41, N 3.02, Ni 46.04. IR (CH_3CN, 293 K) ν_{CO}: 2009(s), 1873(m) cm^{-1}.

4.4 Synthesis of $[NEt_4]_4[H_2Ni_{31}P_4(CO)_{39}]\cdot 2CH_3COCH_3$ and $[NEt_4]_6[H_2Ni_{31}P_4(CO)_{39}]_{0.46}[HNi_{31}P_4(CO)_{39}]_{0.54}[NiCl_4]_{0.46}[BF_4]_{0.54}\cdot 2CH_3COCH_3$

$HBF_4\cdot Et_2O$ (32.5 mg, 0.200 mmol) was added to a solution of $[NEt_4]_6[HNi_{31}P_4(CO)_{39}][Cl]\cdot 2CH_3CN$ (0.68 g, 0.173 mmol) in CH_3CN (20 mL). The resulting mixture was stirred at room temperature for 1 h and, then, the solvent removed *in vacuo*. The residue was washed with H_2O (3×20 mL), thf (3×20 mL), and extracted with acetone (20 mL). Crystals of $[NEt_4]_4[H_2Ni_{31}P_4(CO)_{39}]\cdot 2CH_3COCH_3$ suitable for X-ray analyses were obtained by layering n-hexane (40 mL) on the acetone solution (yield 0.49 g, 77 % based on Ni).

$C_{77}H_{92}N_4Ni_{31}O_{41}P_4$ (3673.44): calcd. C 25.18, H 2.52, N 1.53, Ni 49.54; found: C 25.33, H 2.37, N 1.29, Ni 50.07. IR (CH_3CN, 293 K) ν_{CO}: 2022(s), 1876(m), 1818(w) cm^{-1}.

Crystals of $[NEt_4]_6[H_2Ni_{31}P_4(CO)_{39}]_{0.46}[HNi_{31}P_4(CO)_{39}]_{0.54}[NiCl_4]_{0.46}[BF_4]_{0.54}\cdot 2CH_3COCH_3$ have been obtained with a similar procedure, employing 0.100 mmol of $HBF_4\cdot Et_2O$.

4.5 Oxidation of $[NEt_4]_3[Ni_{11}P(CO)_{18}]$

A solution of PCl_3 (0.014 g, 0.099 mmol) in CH_3CN (5 mL) was added to a solution of $[NEt_4]_3[Ni_{11}P(CO)_{18}]$ (0.44 g, 0.28 mmol) in CH_3CN (15 mL) over a period of 1 h. The resulting mixture was stirred at room temperature for 1 h and, then, the solvent removed *in vacuo*. The residue was washed with H_2O (2×20 mL), thf (2×20 mL), and extracted with CH_3CN (20 mL). The formation of $[HNi_{31}P_4(CO)_{39}]^{5-}$ was confirmed by IR spectroscopy. The reaction can be performed using $[C_7H_7][BF_4]$ instead of PCl_3, and following the same procedure.

IR (CH_3CN, 293 K) ν_{CO}: 2009(s), 1873(m) cm^{-1}.

4.6 Protonation/deprotonation studies of $[H_{6-n}Ni_{31}P_4(CO)_{39}]^{n-}$ (n = 4-6)

(a) The $[HNi_{31}P_4(CO)_{39}]^{5-}$ mono-hydride penta-anion [ν_{CO} 2009(s), 1873(m) cm^{-1} in CH_3CN] may be converted into the $[Ni_{31}P_4(CO)_{39}]^{6-}$ hexa-anion [ν_{CO} 1997(s), 1859(m) cm^{-1} in CH_3CN] after reaction with a base such as CH_3ONa in CH_3CN. In details, CH_3ONa (20 mg, 0.370 mmol) was added as solid to a solution of $[NEt_4]_6[HNi_{31}P_4(CO)_{39}][Cl]\cdot 2CH_3CN$ (0.68 g, 0.173 mmol) in CH_3CN (20 mL) and the solution stirred at room temperature for 1 h. The formation of $[Ni_{31}P_4(CO)_{39}]^{6-}$ was confirmed by IR spectroscopy. $[NEt_4]_6[Ni_{31}P_4(CO)_{39}]$ may be obtained as a solid after removing CH_3CN *in vacuo* from the solution. The reaction may be reversed by adding a strong acid such as $HBF_4\cdot Et_2O$.

(b) The $[HNi_{31}P_4(CO)_{39}]^{5-}$ mono-hydride penta-anion [ν_{CO} 2009(s), 1873(m) cm^{-1} in CH_3CN] may be converted into the $[H_2Ni_{31}P_4(CO)_{39}]^{4-}$ di-hydride tetra-anion [ν_{CO} 2022(s), 1876(m) and 1818(w)cm^{-1} in CH_3CN] after reaction with an acid such as $HBF_4\cdot Et_2O$. In details, $HBF_4\cdot Et_2O$ (32.5 mg, 0.200 mmol) was added to a solution of $[NEt_4]_6[HNi_{31}P_4(CO)_{39}][Cl]\cdot 2CH_3CN$ (0.68 g, 0.173 mmol) in CH_3CN (20 mL) and the solution stirred at room temperature for 1 h. The formation of $[H_2Ni_{31}P_4(CO)_{39}]^{4-}$ was confirmed by IR spectroscopy. The di-hydride tetra-anion was isolated as a crystalline solid following the procedure described in Section 4.4. The reaction may be reversed by adding a base such as CH_3ONa.

4.7 Reaction of $[Ni_{31}P_4(CO)_{39}]^{6-}$ with Na/naphthalene

A solution of Na/naphthalene in dmf was added in small portions to a solution of $[NEt_4]_6[Ni_{31}P_4(CO)_{39}]$ (0.44 g, 0.115 mmol) in dmf (15 mL), and the reaction monitored *via* IR spectroscopy after each addition. The formation of $[Ni_{31}P_4(CO)_{39}]^{7-}$ was confirmed by IR spectroscopy [ν_{CO} 1976(s), 1839(m) cm^{-1} in dmf]. All attempts to isolate the epta-anion as a solid or in a crystalline form failed.

4.8 Electrochemical and spectroelectrochemical studies.

Electrochemical measurements were recorded on a Princeton Applied Research (PAR) 273A Potentiostat/Galvanostat, interfaced to a computer employing PAR M270 electrochemical software, and were performed in CH_3CN solutions containing $[N^nBu_4][PF_6]$ (0.1 mol dm^{-3}) as the supporting electrolyte at room temperature (20±5 °C). HPLC grade CH_3CN (Sigma-Aldrich) was stored under argon over 3-Å molecular sieves. Electrochemical grade $[N^nBu_4][PF_6]$ was purchased from Fluka and used without further purification. Cyclic voltammetry was performed in a three-electrode cell, having a platinum-disc working electrode, a platinum-spiral counter electrode and a Ag/AgCl(aq) reference electrode mounted with a salt bridge containing the

$CH_3CN/[N^nBu_4][PF_6]$ electrolyte and separated by a Vycor frit. Under the present experimental conditions, the one-electron oxidation of ferrocene occurs at E° = +0.45 V *vs* Ag/AgCl.

Infrared (IR) spectroelectrochemical measurements were carried out using an optically transparent thin-layer electrochemical (OTTLE) cell equipped with CaF_2 windows, platinum mini-grid working and auxiliary electrodes and silver wire pseudo-reference electrode.[66] During the microelectrolysis procedures, the electrode potential was controlled by a Princeton Applied Research (PAR) 273A Potentiostat/Galvanostat, interfaced to a computer employing PAR M270 electrochemical software. Argon-saturated CH_3CN solutions of the compound under study, containing $[N^nBu_4][PF_6]$ 0.1 M as the supporting electrolyte, were used. The *in situ* spectroelectrochemical experiments have been performed by collecting spectra of the solution at constant time intervals during the oxidation or reduction obtained by continuously increasing or lowering the initial working potential at a scan rate of 0.5 mV/sec. IR spectra were recorded on a Perkin-Elmer FT-IR 1725X spectrophotometer.

4.9 X-ray Crystallographic Study.

Crystal data and collection details for $[NEt_4]_3[Ni_{11}P(CO)_{18}]$, $[NEt_4]_4[H_2Ni_{31}P_4(CO)_{39}]\cdot 2CH_3COCH_3$, $[NEt_4]_6[HNi_{31}P_4(CO)_{39}][Cl]\cdot 2CH_3CN$ and $[NEt_4]_6[H_2Ni_{31}P_4(CO)_{39}]_{0.46}[HNi_{31}P_4(CO)_{39}]_{0.54}[NiCl_4]_{0.46}[BF_4]_{0.54}\cdot 2CH_3COCH_3$, are reported in Table S.1. The diffraction experiments were carried out on a Bruker APEX II diffractometer equipped with a CCD detector using Mo–Kα radiation. Data were corrected for Lorentz polarization and absorption effects (empirical absorption correction SADABS).[67] Structures were solved by direct methods and refined by full-matrix least-squares based on all data using F^2.[68] Hydrogen atoms were fixed at calculated positions and refined by a riding model. All non-hydrogen atoms were refined with anisotropic displacement parameters, unless otherwise stated.

$[NEt_4]_3[Ni_{11}P(CO)_{18}]$: The asymmetric unit of the unit cell contains one cluster anion and three $[NEt_4]^+$ cations (all located on general positions). Two $[NEt_4]^+$ cations are disordered and, thus, they have been split into two positions and refined with one occupancy parameter per disordered group. Similar *U* parameter restraints have been applied to the $[NEt_4]^+$ cations (SIMU command in SHELXL, s.u. 0.05).Restraints to bond distances were applied as follow (s.u. 0.05): 1.45 Å for C–N and 1.54 Å for C–C in the disordered $[NEt_4]^+$.

$[NEt_4]_4[Ni_{31}P_4(CO)_{39}]\cdot 2CH_3COCH_3$: The asymmetric unit of the unit cell contains half of a cluster anion (on a 2-axis), two $[NEt_4]^+$ cations (on general positions) and one CH_3COCH_3 molecule (on a general positions). One Ni(CO) group and three CO ligands in the cluster anion, the two $[NEt_4]^+$ cations and the CH_3COCH_3 molecule are disordered and, thus, they have been split into two

positions each and refined with one occupancy parameter per disordered group. Similar *U* parameter restraints have been applied to the $[NEt_4]^+$ cations and the CH_3COCH_3 molecule (SIMU command in SHELXL, s.u. 0.02).Restraints to bond distances were applied as follow (s.u. 0.03): 1.45 Å for C–N and 1.54 Å for C–C in $[NEt_4]^+$; 1.28 Å for C–O and 1.45 Å for C–C in CH_3COCH_3.

$[NEt_4]_6[Ni_{31}P_4(CO)_{39}][Cl]\cdot 2CH_3CN$: The asymmetric unit of the unit cell contains one cluster anion, one chloride anion, six $[NEt_4]^+$ cations and two CH_3CN molecules (all located on general positions). Similar *U* parameter restraints have been applied to all the C, N and O(SIMU command in SHELXL, s.u. 0.01). The C-C distances of the $[NEt_4]^+$ cations have been restrained to be similar (SADI command in SHELXL, s.u. 0.02). The quality of the crystals is not very good and, thus, some ALERT A messages remain in the checkcif. Nonetheless, the overall structure and connectivity of the cluster can be safely deduced and compares very well with the other two structures herein reported.

$[NEt_4]_6[H_2Ni_{31}P_4(CO)_{39}]_{0.46}[HNi_{31}P_4(CO)_{39}]_{0.54}[NiCl_4]_{0.46}[BF_4]_{0.54}\cdot 2CH_3COCH_3$: The asymmetric unit of the unit cell contains half of a cluster anion (on a 2-axis), three $[NEt_4]^+$ cations (on general positions), one CH_3COCH_3 molecule (on a general positions), half of a $[NiCl_4]^{2-}$ and half of a $[BF_4]^-$ anions (on 2-axes and disordered). Similar *U* parameter restraints have been applied to all the atoms(SIMU command in SHELXL, s.u. 0.008).

ASSOCIATED CONTENT

Supporting Information

Crystallographic data in CIF format. Supplementary electrochemical and spectroelectrochemical data. Crystal data and experimental details for $[NEt_4]_3[Ni_{11}P(CO)_{18}]$, $[NEt_4]_4[Ni_{31}P_4(CO)_{39}]\cdot 2CH_3COCH_3$, $[NEt_4]_6[Ni_{31}P_4(CO)_{39}][Cl]\cdot 2CH_3CN$ and $[NEt_4]_6[H_2Ni_{31}P_4(CO)_{39}]_{0.46}[HNi_{31}P_4(CO)_{39}]_{0.54}[NiCl_4]_{0.46}[BF_4]_{0.54}\cdot 2CH_3COCH_3$.

Accession Codes

CCDC 1577648-1577651 contain the supplementary crystallographic data for this paper. These data can be obtained free of charge via www.ccdc.cam.ac.uk/data_request/cif, or by emailing data_request@ccdc.cam.ac.uk, or by contacting The Cambridge Crystallographic Data Centre, 12, Union Road, Cambridge CB2 1EZ, UK; fax: +44 1223 336033.

AUTHOR INFORMATION

Corresponding Author

* E-mail: stefano.zacchini@unibo.it. Tel: +39 051 2093711. Web: https://www.unibo.it/sitoweb/stefano.zacchini/en.

Notes

The authors declare no competing financial interest.

ACKNOWLEDGMENTS

We thank the Ministero dell'Università e della Ricerca Scientifica e Tecnologica (MIUR), and the University of Bologna for financial support.

REFERENCES

1 Prins, R.; Bussell, M. E. Metal Phosphides: Preparation, Characterization and Catalytic Reactivity. *Catal. Lett.* **2012**, *142*, 1413.

2 Alexander, A.-M.; Hargreaves, J. S. J. Alternative catalytic materials: carbides, nitrides, phosphides and amorphous boron alloys. *Chem. Soc. Rev.* **2010**, *39*, 4388.

3 Yang, S.; Liang, C.; Prins, R. A novel approach to synthesizing highly active Ni_2P/SiO_2 hydrotreating catalysis. *J. Catal.* **2006**, *237*, 118.

4 Huang, Z.; Chen, Z.; Chen, Z.; Lv, C.; Meng, H.; Zhang, C. $Ni_{12}P_5$ Nanoparticles as an Efficient Catalyst for Hydrogen Generation *via* Electrolysis and Photoelectrolysis. *ACS Nano* **2014**, *8*, 8121.

5 Popczun, E. J.; McKone, J. R.; Read, C. G.; Biacchi, A. J.; Wiltrout, A. M.; Lewis, N. S.; Schaak, R. E. Nanostructured Nickel Phosphides as an Electrocatalyst for the Hydrogen Evolution Reaction. *J. Am. Chem. Soc.* **2013**, *135*, 9267.

6 Zou, X.; Zhang, Y. Noble metal-free hydrogen evolution catalysts for water splitting. *Chem. Soc. Rev.* **2015**, *44*, 5148.

7 (a) Pu, Z.; Liu, Q.; Tang, C.; Asiri, A. M.; Sun, X. Ni_2P nanoparticle films supported on a Ti plate as an efficient hydrogen evolution cathode. *Nanoscale* **2014**, *6*, 11031. (b) Kucernak, A. R. J.; Sundaram, V. N. N. Nickel phosphide: the effect of phosphorus content on hydrogen evolution activity and corrosion resistance in acidic medium. *J. Mater. Chem. A* **2014**, *2*, 17435.

8 Gillot, F.; Boyanov, S.; Dupont, L.; Doublet, M.–L.; Morcrette, M.; Monconduit, L.; Tarascon, J.–M. Electrochemical Reactivity and Design of Ni_2P Negative Electrodes for Secondary Li-Ion Batteries. *Chem. Mater.* **2005**, *17*, 6327.

9 Greenwood, N. N.; Earnshaw, A. Chemistry of the Elements. **1984**, Pergamon Press Plc, 1st ed, ISBN 0-08-022057-6.

10 Schmetterer, C.; Vizdal, J.; Ipser, H. A new investigation of the system Ni-P. *Intermetallics* **2009**, *17*, 826.

11 (a) Aronsson, B. The crystal structure of Ni_3P. (Fe_3P-Type). *Acta Chem. Scand.* **1955**, *9*, 137. (b) Rundqvist, S.; Hassler, E.; Lundvik, L. Refinement of the Ni_3P structure. *Acta Chem. Scand.* **1962**, *16*, 242.

12 (a) Oryshchyn, S.; Babizhetskyy, V.; Chykhriy, S.; Aksel'rud, L.; Stoyko, S.; Bauer, J.; Guérin, R.; Kuz'ma, Yu. Crystal Structure of Ni_5P_2. *Inorg. Mater.* **2004**, *40*, 380. (b) Saini, G. S.; Calvert, L. D.; Taylor, J. B. Compounds of the type M_5X_2: Pd_5As_2, Ni_5Si_2 and Ni_5P_2. *Canad. J. Chem.* **1964**, *42*, 1511.

13 (a) Elfström, M. The crystal structure of Ni_5P_4. *Acta Chem. Scand.* **1965**, *19*, 1694. (b) Donohue, P. C.; Bither, T. A.; Sargent Young, H. High-pressure synthesis of pyrite-type nickel diphosphide and nickel diarsenide. *Inorg. Chem.* **1968**, *7*, 998.

14 Zacchini, S. Using Metal Carbonyl Clusters To Develop a Molecular Approach towards Metal Nanoparticles. *Eur. J. Inorg. Chem.* **2011**, 4125.

15 Jin, R.; Zeng, C.; Zhou, M.; Chen, Y. Atomically Precise Colloidal Metal Nanoclusters and Nanoparticles: Fundamentals and Opportunities. *Chem. Rev*. **2016**, *116*, 10346.

16 Buchwalter, P.; Rosé, J.; Braunstein, P. Multimetallic Catalysis Based on Heterometallic Complexes and Clusters. *Chem. Rev.* **2015**, *115*, 28.

17 (a) Adams, R. D.; Captain, B. Bimetallic cluster complexes: synthesis, structures and applications to catalysis. *J. Organomet. Chem.* **2004**, *689*, 4521. (b) Adams, R. D. Metal segregation in bimetallic clusters and its possible role in synergism and bifunctional catalysis. *J. Organomet. Chem.* **2000**, *600*, 1. (c) Vidick, D.; Ke, X.; Devillers, M.; Poleunis, C.; Delcorte, A.; Moggi, P.; Van Tendeloo, G.; Hermans, S. Heterometal nanoparticles from Ru-based molecular clusters covalently anchored onto functionalized carbon nanotubes and nanofibers. *Beilstein J. Nanotechnol.* **2015**, *6*, 1287.

18 (a) *Catalysis by Di- and Polynuclear Metal Cluster Complexes*. Adams, R. D.; Cotton, F. A., Eds.; Wiley-VCH, New York, 1998. (b) Johnson, B. F. G. Nanoparticles in Catalysis. *Top. Catal.* **2003**, *24*, 147. (c) Jones, M. D.; Duer, M. J.; Hermans, S.; Khimyak, Y. Z.; Johnson, B. F. G.; Thomas, J. M. Solid-state NMR studies of MCM-41 supported with a highly catalytically active cluster. *Angew. Chem. Int. Ed.* **2002**, *41*, 4726.

19 (a) Adams, R. D.; Trufan, E. Ruthenium-tin cluster complexes and their applications as bimetallic nanoscale heterogeneous hydrogenation catalysts. *Phil. Trans. R. Soc. A* **2010**, *368*, 1473. (b) Schweyer-Tihay, F.; Estournès, C.; Braunstein, P.; Guille, J.; Paillaud, J. L.; Richard-Plouet, M.; Rosé, J. On the nature of metallic nanoparticles obtained from

molecular Co_3Ru-carbonyl clusters in mesoporous silica matrices. *Phys. Chem. Chem. Phys.* **2006**, *8*, 4018. (c) Schweyer, F.; Braunstein, P.; Estournès, C.; Guille, J.; Kessler, H.; Paillaud, J. L.; Rosé, J. Metallic nanoparticles from heterometallic Co-Ru carbonyl clusters in mesoporous silica xerogels and MCM-41-type materials. *Chem. Commun.* **2000**, 1271.

20 (a) Robinson, I.; Zacchini, S.; Tung, L. D.; Maenosono, S.; Thanh, N. T. K. Synthesis and Characterization of Magnetic Nanoalloys from Bimetallic Carbonyl Clusters. *Chem. Mater.* **2009**, *21*, 3021. (b) Albonetti, S.; Bonelli, R.; Epoupa Mengou, J.; Femoni, C.; Tiozzo, C.; Zacchini, S.; Trifirò, F. Gold/iron carbonyl clusters as precursors for TiO_2 supported catalysts. *Catal. Today* **2008**, *137*, 483. (c) Albonetti, S.; Bonelli, R.; Delaigle, R.; Femoni, C.; Gaigneaux, E. M.; Morandi, V.; Ortolani, L.; Tiozzo, C.; Zacchini, S.; Trifirò, F. Catalytic combustion of toluene over cluster-derived gold/iron catalysts. *Appl. Catal. A* **2010**, *372*, 138.

21 (a) Bonelli, R.; Albonetti, S.; Morandi, V.; Ortolani, L.; Riccobene, P. M.; Scirè, S.; Zacchini, S. Design of nano-sized FeO_x and Au/FeO_x catalysts supported on CeO_2 for total oxidation of VOC. *Appl. Catal. A* **2011**, *395*, 10. (b) Bonelli, R.; Lucarelli, C.; Pasini, T.; Liotta, L. F.; Zacchini, S.; Albonetti, S. Total oxidation of volatile organic compounds on Au/FeO_x catalysts supported on mesoporous SBA-15 silica. *Appl. Catal. A* **2011**, *400*, 54. (c) Bonelli, R.; Zacchini, S.; Albonetti, S. Gold/Iron Carbonyl Clusters for Tailored Au/FeO_x Supported Catalysts. *Catalysys* **2012**, *2*, 1.

22 (a) Bortoluzzi, M.; Ceriotti, A.; Ciabatti, I.; Della Pergola, R.; Femoni, C.; Iapalucci, M. C.; Storione, A.; Zacchini, S. Platinum carbonyl clusters stabilized by Sn(II)-based fragments: syntheses and structures of $[Pt_6(CO)_6(SnCl_2)(SnCl_3)_4]^{4-}$, $[Pt_9(CO)_8(SnCl_2)_3(SnCl_3)_2(Cl_2SnOCOSnCl_2)]^{4-}$ and $[Pt_{10}(CO)_{14}\{Cl_2Sn(OH)SnCl_2\}_2]^{2-}$. *Dalton Trans.* **2016**, *45*, 5001. (b) Ciabatti, I.; Femoni, C.; Gaboardi, M.; Iapalucci, M. C.; Longoni, G.; Pontiroli, D.; Riccò, M.; Zacchini, S. Structural rearrangements induced by acid-base reactions in metal carbonyl clusters: the case of $[H_{3-n}Co_{15}Pd_9C_3(CO)_{38}]^{n-}$ (n = 0-3). *Dalton Trans.* **2014**, *43*, 4388. (c) Ciabatti, I.; Femoni, C.; Iapalucci, M. C.; Longoni, G.; Zacchini, S.; Zarra, S. Surface decorated platinum carbonyl clusters. *Nanoscale* **2012**, *4*, 4166.

23 (a) Ciabatti, I.; Femoni, C.; Iapalucci, M. C.; Longoni, G.; Zacchini, S. Platinum Carbonyl Clusters Chemistry: Four Decades of Challenging Nanoscience. *J. Clust. Sci.* **2014**, *25*, 115. (b) Bernardi, A.; Ciabatti, I.; Femoni, C.; Iapalucci, M. C.; Longoni, G.; Zacchini, S. Ni-Cu tetracarbide carbonyls with vacant Ni(CO) fragments as borderline compounds between molecular and quasi-molecular clusters. *Dalton Trans.* **2013**, *42*, 407. (c) Cattabriga, E.;

Ciabatti, I.; Femoni, C.; Funaioli, T.; Iapalucci, M. C.; Zacchini, S. Syntheses, Structures, and Electrochemistry of the Defective *ccp* $[Pt_{33}(CO)_{38}]^{2-}$ and the *bcc* $[Pt_{40}(CO)_{40}]^{6-}$ Molecular Nanoclusters. *Inorg. Chem.* **2016**, *55*, 6068.

24 (a) Li, C.; Leong, W. K. The deposition of osmium carbonyl clusters onto inorganic oxide surfaces: A ToF-SIMS and IR spectroscopic study of the surface species. *J. Colloid Interface Sci.* **2008**, *328*, 29. (b) Gutmann, T.; Walaszek, B.; Yeping, X.; Wächtler, M.; del Rosal, I.; Grünberg, A.; Poteau, R.; Axet, R.; Lavigne, G.; Chaudret, B.; Limbach, H.–H.; Buntkowsky, G. Hydrido-Ruthenium Cluster Complexes as Models for Reactive Surface Hydrogen Species of Ruthenium Nanoparticles. Solid-State ^{2}H NMR and Quantum Chemical Calculations. *J. Am. Chem. Soc.* **2010**, *132*, 11759. (c) Yamazoe, S.; Koyasu, K.; Tsukuda, T. Nonscalable Oxidation Catalysis of Gold Clusters. *Acc. Chem. Res.* **2014**, *47*, 816.

25 (a) *Metal Clusters in Chemistry*. Braunstein, P.; Oro, L. A.; Raithby, P. Eds.; Wiley-VCH, Weinheim, Germany, 1999. (b) *Clusters and Colloids*. Schmid, G. Ed.; VCH, Weinheim, Germany, 1994.

26 (a) Schmid, G.; Fenske, D. Metal clusters and nanoparticles: Introduction. *Philos. Trans. R. Soc., A* **2010**, *368*, 1207. (b) Taketoshi, A.; Haruta, M. Size- and Structure-specificity in Catalysis by Gold Clusters. *Chem. Lett.* **2014**, *43*, 380.

27 (a) Raithby, P. R. The Build-Up of Bimetallic Transition Metal Clusters. *Platinum Metal. Rev.* **1998**, *42*, 146. (b) Johnson, B. F. G. From clusters to nanoparticles and catalysis. *Coord. Chem. Rev.* **1999**, *190-192*, 1269. (c) Hogarth, G.; Kabir, S. E.; Nordlander, E. Cluster chemistry in the Noughties: new developments and their relationship to nanoparticles. *Dalton Trans.* **2010**, *39*, 6153.

28 (a) Mednikov, E. G.; Dahl, L. F. Crystallographically Proven Nanometer-Sized Gold Thiolate Cluster $Au_{102}(SR)_{44}$: Its Unexpected Molecular Anatomy and Resulting Stereochemical and Bonding Consequences. *Small* **2008**, *4*, 534. (b) Mednikov, E. G.; Dahl, L. F. Syntheses, structures and properties of primarily nanosized homo/heterometallic palladium CO/PR_3-ligated clusters. *Phil. Trans. R. Soc. A* **2010**, *368*, 23.

29 Femoni, C.; Iapalucci, M. C.; Kaswalder, F.; Longoni, G.; Zacchini, S. The possible role of metal carbonyl clusters in nanoscience and nanotechnologies. *Coord. Chem. Rev*. **2006**, *250*, 1580.

30 (a) Masters, A. F.; Meyer, J. T. Structural systematic in nickel carbonyl cluster anions. *Polyhedron* **1995**, *14*, 339. (b) Battie, J. K.; Masters, A. F.; Meyer, J. T. Nickel carbonyl cluster complexes. *Polyhedron* **1995**, *14*, 829.

31 (a) Bernardi, A.; Ciabatti, I.; Femoni, C.; Iapalucci, M. C.; Longoni, G.; Zacchini, S. Molecular nickel poly-carbide carbonyl nanoclusters: The octa-carbide $[HNi_{42}C_8(CO)_{44}(CuCl)]^{7-}$ and the deca-carbide $[Ni_{45}C_{10}(CO)_{46}]^{6-}$. *J. Organomet. Chem.* **2016**, *812*, 229-239. (b) Ciabatti, I.; Femoni, C.; Funaioli, T.; Iapalucci, M. C.; Merighi, S.; Zacchini, S. The redox chemistry of $[Ni_9C(CO)_{17}]^{2-}$ and $[Ni_{10}(C_2)(CO)_{16}]^{2-}$: Synthesis, electrochemistry and structure of $[Ni_{12}C(CO)_{18}]^{4-}$ and $[Ni_{22}(C_2)_4(CO)_{28}(Et_2S)]^{2-}$. *J. Organomet. Chem.* **2017**, *849-850*, 299. (c) Bortoluzzi, M.; Ciabatti, I.; Femoni, C.; Hayatifar, M.; Iapalucci, M. C.; Longoni, G.; Zacchini, S. Peraurated nickel carbide carbonyl clusters: the cationic $[Ni_6(C)(CO)_8(AuPPh_3)_8]^{2+}$ monocarbide and the $[Ni_{12}(C)(C_2)(CO)_{17}(AuPPh_3)_3]^{-}$ anion containing one carbide and one acetylide unit. *Dalton Trans.* **2014**, *43*, 13471.

32 (a) Ciabatti, I.; Fabrizi de Biani, F.; Femoni, C.; Iapalucci, M. C.; Longoni, G.; Zacchini, S. Selective synthesis of the $[Ni_{36}Co_8C_8(CO)_{48}]^{6-}$ octa-carbide carbonyl cluster by thermal decomposition of the $[H_2Ni_{22}Co_6C_6(CO)_{36}]^{4-}$ hexa-carbide. *Dalton Trans.* **2013**, *42*, 9662. (b) Ciabatti, I.; Femoni, C.; Iapalucci, M. C.; Ienco, A.; Longoni, G.; Manca, G.; Zacchini, S. Intramolecular d^{10}-d^{10} Interactions in a $Ni_6C(CO)_9(AuPPh_3)_4$ Bimetallic Nickel-Gold Carbide Carbonyl Cluster. *Inorg. Chem.* **2013**, *52*, 10559. (c) Ciabatti, I.; Femoni, C.; Iapalucci, M. C.; Longoni, G.; Zacchini, S. Bimetallic Nickel-Cobalt Hexacarbido Carbonyl Clusters $[H_{6-n}Ni_{22}Co_6C_6(CO)_{36}]^{n-}$ (n = 3-6) Possessing Polyhydride Nature and Their Base-Induced Degradation to the Monoacetylide $[Ni_9CoC_2(CO)_{16-x}]^{3-}$ (x = 0, 1). *Organometallics* **2012**, *31*, 4593.

33 Femoni, C.; Iapalucci, M. C.; Longoni, G.; Zacchini, S. Icosahedral Ga-Centred Nickel Carbonyl Clusters: Synthesis and Characterization of $[H_{3-n}Ni_{12}(\mu_{12}\text{-Ga})(CO)_{22}]^{n-}$ (n = 2, 3) and $[Ni_{14.3}(\mu_{12}\text{-Ga})(CO)_{24.3}]^{3-}$ anions. *Eur. J. Inorg. Chem.* **2010**, 1056.

34 Ceriotti, A.; Demartin, F.; Heaton, B. T.; Ingallina, P.; Longoni, G.; Manassero, M.; Marchionna, M.; Masciocchi, N. Nickel carbonyl clusters containing interstitial carbon-congener atoms: synthesis and structural characterization of the $[Ni_{12}(\mu_{12}\text{-E})(CO)_{22}]^{2-}$ (E = Ge, Sn) and $[Ni_{10}(\mu_{10}\text{-Ge})(CO)_{20}]^{2-}$ dianions. *J. Chem. Soc., Chem. Commun.* **1989**, 786.

35 Albano, V. G.; Demartin, F.; Iapalucci, M. C.; Longoni, G.; Monari, M.; Zanello, P. New icosahedral heterometallic nickel carbonyl clusters containing bismuth. *J. Chem. Soc. Dalton Trans.* **1992**, 497.

36 Albano, V. G.; Demartin, F.; Femoni, C.; Iapalucci, M. C.; Longoni, G.; Monari, M.; Zanello, P. Synthesis and characterization of new paramagnetic nickel carbonyl clusters

containing antimony atoms: X-ray structure of $[NEt_3CH_2Ph]_2[Ni_{15}(\mu_{12}\text{-}Sb)(CO)_{24}]$ and $[NEt_4]_3[Ni_{10}Sb_2(\mu_{12}\text{-}Ni)(CO)_{18}]$. *J. Organomet. Chem.* **2000**, *593-594*, 325.

37 Femoni, C.; Iapalucci, M. C.; Longoni, G.; Svensson, P. H. A high-nuclearity Ni-Sb carbonyl cluster displaying unprecedented metal stereochemistries: synthesis and X-ray structure of $[NEt_4]_6[Ni_{31}Sb_4(CO)_{40}]\cdot 2Me_2CO$. *Chem. Commun.* **2000**, 655.

38 Albano, V. G.; Demartin, F.; Iapalucci, M. C.; Laschi, F.; Longoni, G.; Sironi, A.; Zanello, P. Icosahedral carbonyl clusters $[Ni_{10}Sb_2(\mu_{12}\text{-}Ni)\{Ni(CO)_3\}_2(CO)_{18}]^{n-}$ (n = 2, 3 or 4); synthesis, spectroscopic, electrochemical and bonding analysis. Crystal structures of $[Ni_{10}Sb_2(\mu_{12}\text{-}Ni)\{Ni(CO)_3\}_2(CO)_{18}]^{n-}$ (n = 2 or 3). *J. Chem. Soc., Dalton Trans*. **1991**, 739.

39 Femoni, C.; Iapalucci, M. C.; Longoni, G.; Zacchini, S.; Ciabatti, I.; Della Valle, R. G.; Mazzani, M.; Riccò, M. The Chemistry of Ni-Sb Carbonyl Clusters - Synthesis and Characterization of the $[Ni_{19}Sb_4(CO)_{26}]^{4-}$ Tetraanion and the Viologen Salts of $[Ni_{13}Sb_2(CO)_{24}]^{n-}$ Carbonyl Clusters. *Eur. J. Inorg. Chem.* **2014**, 4151.

40 (a) Esenturk, E. N.; Fettinger, J.; Eichhorn, B. Synthesis and characterization of the $[Ni_6Ge_{13}(CO)_5]^{4-}$ and $[Ge_9Ni_2(PPh_3)]^{2-}$ Zintl ion clusters. *Polyhedron* **2006**, *25*, 521. (b) Perla, L. G.; Sevov, S. C. $[Bi_{12}Ni_7(CO)_4]^{4-}$: Aggregation of Intermetalloid Clusters by Their Thermal Deligation and Oxidation. *Inorg. Chem.* **2015**, *54*, 8401.

41 Goicoechea, J. M.; Hull, M. W.; Sevov, S. C. Heteroatomic Deltahedral Clusters: Synthesis and Structures of *closo*-$[Bi_3Ni_4(CO)_6]^{3-}$, *closo*-$[Bi_4Ni_4(CO)_6]^{2-}$, the Open Cluster $[Bi_3Ni_6(CO)_9]^{3-}$, and the Intermetalloid *closo*-$[Ni_x@\{Bi_6Ni_6(CO)_8\}]^{4-}$. *J. Am. Chem. Soc.* **2007**, *129*, 7885.

42 (a) Mlynek, P. D.; Dahl, L. F. New Nickel-Antimony Carbonyl Clusters: Stereochemical Analyses of the $[Ni_{10}(SbR)_2(CO)_{18}]^{2-}$ Dianions (R = Me, Et, ^{i}Pr, ^{t}Bu, *p*-FC_6H_4) Containing Empty 1,12-$Ni_{10}Sb_2$ Icosahedral Cages and of the Unprecedented Stibinido-Bridged 34-Electron $Ni_2(CO)_4(\mu_2\text{-}Sb^tBu_2)_2$ Dimer. *Organometallics*, **1997**, *16*, 1641. (b) Mlynek, P. D.; Dahl, L. F. New Noncentered Icosahedral Nickel-Bismuth Carbonyl Clusters: Geometric Analysis of the Homologous $[Ni_{10}(EMe)_2(CO)_{18}]^{2-}$ Dianions (E = P, As, Sb, Bi) Containing Noncentered 1,12-$Ni_{10}E_2$ Icosahedral Cages.. *Organometallics*, **1997**, *16*, 1655.

43 (a) Zebrowski, J. P.; Hayashi, R. K.; Bjarnason, A.; Dahl, L. F. A New Family of 14-Vertex Hexacapped Metal Cubes with Main Group IV (14) Atoms: Synthesis and Structural-Bonding Analysis of $Ni_9(\mu_4\text{-}GeEt)_6(CO)_8$ Containing a Nickel-Centered $Ni_8(\mu_4\text{-}Ge)_6$ Cubic Cage with an Unusual Electron Count. *J. Am. Chem. Soc.* **1992**, *114*, 3121. (b) Zebrowski, J. P.; Hayashi, R. K.; Dahl, L. F. A New Family of Icosahedral Cages with Transition Metal and Main Group IV (14) Atoms: Synthesis and Structural-Bonding Analysis of the

$[Ni_{11}(SnR)_2(CO)_{18}]^{2-}$ Dianions (R = ^{n}Bu, Me) Containing Ni-Centered Icosahedral $Ni_{10}Sn_2$ Cages and of Their Unusual $[Ni(SnRCl_2)_4(CO)]^{2-}$ Precursors Containing a Trigonal-Bipyramidal d^8 Nickel(II) Configuration. *J. Am. Chem. Soc.* **1993**, *115*, 1142.

44 DesEnfants, II, R. E.; Gavney, Jr., J. A.; Hayashi, R. K.; Rae, A. D.; Dahl, L. F.; Bjarnason, A. Reactions of the $[Ni_6(CO)_{12}]^{2-}$ dianion with stibine and bismuthine reagents: synthesis and stereophysical characterization of the $[Ni_{10}(SbPh)_2(CO)_{18}]^{2-}$ dianion containing a noncentered icosahedral $Ni_{10}Sb_2$ core and $Ni_2(CO)_4(\mu_2\text{-}Ph_2SbOSbPh_2)_2$ containing a centrosymmetric eight-membered $(NiSbOSb)_2$ ring. *J. Organomet. Chem.* **1990**, *383*, 543.

45 (a) Colbran, S. B.; Hay, C. M.; Johnson, B. F. G.; Lahoz, F. J.; Lewis, J.; Raithby, P. R. Synthesis, characterization, and reactivity of transition metal carbonyl clusters containing an interstitial phosphorus in a trigonal co-ordination environment: the X-ray structures of $[PPh_3Me][Os_6(CO)_{18}P]$ and $[Os_6(CO)_{18}P(AuPPh_3)]$. *J. Chem. Soc., Chem. Commun.* **1986**, 1766. (b) Colbran, S. B.; Lahoz, F. J.; Raithby, P. R.; Lewis, J.; Johnson, B. F. G.; Cardin, C. J. Stepwise construction of $[Os_6(CO)_{18}(\mu_6\text{-}P)]^-$, a hexanuclear osmium cluster monoanion with trigonal-prismatic co-ordination for phosphorus: X-ray crystal structures of $[Os_6(\mu\text{-}H)_2(CO)_{20}(MeCN)(\mu_3\text{-}PH)]$ and $[PPh_3Me][Os_6(CO)_{18}(\mu_6\text{-}P)]$. *J. Chem. Soc., Dalton Trans.* **1988**, 173. (c) Colbran, S. B.; Housecroft, C. E.; Johnson, B. F. G.; Lewis, J.; Owen, S. M.; Raithby, P. R. An X-ray crystal and electronic structural investigation of the interstitial phosphide cluster $[Os_6(CO)_{18}PCl]$. *Polyhedron*, **1988**, *7*, 1759.

46 Randles, M. D.; Willis, A. C.; Cifuentes, M. P.; Humphrey, M. G. High-nuclearity ruthenium carbonyl cluster chemistry. 8: Phosphine activation, CO insertion, and deruthenation at a phosphido cluster. X-ray structures of $[PPN][Ru_8(\mu_8\text{-}P)(\mu\text{-}CO)_2(CO)_{20}]$ and $[PPN][Ru_7(\mu_7\text{-}P)(\mu\text{-}\eta_2\text{-}OCPh_2)(\mu\text{-}PPh_2)(\mu\text{-}CO)(CO)_{17}]$. *J. Organomet. Chem.* **2007**, *692*, 4467.

47 (a) Cifuentes, M. P.; Waterman, S. M.; Humphrey, M. G.; Heath, G. A.; Skelton, B. W.; White, A. H.; Perera, M. P. S.; Williams, M. L. High nuclearity ruthenium carbonyl cluster chemistry VII. Synthesis, NMR studies, electrochemistry and X-ray crystal structure of $[PPN][Ru_8(\mu_8\text{-}P)(CO)_{22}]$. *J. Organomet. Chem.* **1998**, *565*, 193. (b) Randles, M. D.; Willis, A. C.; Cifuentes, M. P.; Humphrey, M. G. Bis(triphenylphosphoranylidene)ammonium docosacarbonyl(μ_8-phosphido)octaruthenate chloroform solvate. *Acta Crystallogr., Sect. E* **2006**, *62*, m2350.

48 (a) Vidal, J. L. ; Walker, W. E.; Pruett, R. L.; Schoening, R. C. $[Rh_9P(CO)_{21}]^{2-}$. Example of encapsulation of phosphorus by transition-metal-carbonyl clusters. *Inorg. Chem.* **1979**, *18*, 129. (b) Vidal, J. L.; Walker, W. E.; Schoening, R. C. $[Rh_{10}P(CO)_{23}]^{3-}$. A transition-metal

carbonyl cluster with a metal polyhedron based on the bicapped square antiprism as illustrated by the structural study of the benzyltriethylammonium salt. *Inorg. Chem.* **1981**, *20*, 238.

49 Ragaini, F.; Sironi, A.; Fumagalli, A. Deactivation of a $[PPN^+][Rh(CO)_4]$-based catalytic system [PPN = $(PPh_3)_2N^+$]. The first decomposition reaction of PPN^+ and the formation of $[Rh_{10}P(CO)_{22}]^{3-}$. *Chem. Commun.* **2000**, 2117.

50 Ciani, G.; Sironi, A.; Martinengo, S.; Garlaschelli, L.; Della Pergola, R.; Zanello, P.; Laschi, F.; Masciocchi, N. Synthesis and X-ray Characterization of the Phosphido-Carbonyl Cluster Anions $[Co_9(\mu_8\text{-}P)(CO)_{21}]^{2-}$ and $[Co_{10}(\mu_8\text{-}P)(CO)_{23}]^{3-}$. *Inorg. Chem.* **2001**, *40*, 3905.

51 Dreher, C.; Zabel, M.; Bodensteiner, M.; Scheer, M. $[(CO)_4W(PH_3)_2]$ as a Source of Semi-interstitial Phosphorus Ligands in Cobalt Carbonyl Clusters. *Organometallics* **2010**, *29*, 5187.

52 Hong, C. S.; Berben, L. A.; Long, J. R. Synthesis and characterization of a decacobalt carbonyl cluster with two semi-interstitial phosphorus atoms. *Dalton Trans.* **2003**, 2119.

53 (a) Chini, P.; Ciani, G.; Martinengo, S.; Sironi, A.; Longhetti, L.; Heaton, B. T. Synthesis and X-ray crystal structure of the anion $[Co_6(CO)_{14}(\mu\text{-}CO)_2P]^-$; an example of a 'semi-interstitial phosphide'. *J. Chem. Soc., Chem. Commun.* **1979**, 188. (b) Ciani, G.; Sironi, A. Crystal and molecular structure of the anion phosphido-di-μ-carbonyltetradecacarbonyl hexacobaltate(1–) in its tetraphenylphosphonium salt. *J. Organomet. Chem.* **1983**, *241*, 385.

54 (a) Bortoluzzi, M.; Ciabatti, I.; Femoni, C.; Funaioli, T.; Hayatifar, M.; Iapalucci, M. C.; Longoni, G.; Zacchini, S. Homoleptic and heteroleptic Au(I) complexes containing the new $[Co_5C(CO)_{12}]^-$ cluster as ligand. *Dalton Trans.* **2014**, *43*, 9633. (b) Ciabatti, I.; Femoni, C.; Hayatifar, M.; Iapalucci, M. C.; Ienco, A.; Longoni, G.; Manca, G.; Zacchini, S. Octahedral Co-Carbide Carbonyl Clusters Decorated by $[AuPPh_3]^+$ Fragments: Synthesis, Structural Isomerism, and Aurophilic Interactions of $Co_6C(CO)_{12}(AuPPh_3)_4$. *Inorg. Chem.* **2014**, *53*, 9761. (c) Ciabatti, I.; Femoni, C.; Hayatifar, M.; Iapalucci, M. C.; Longoni, G.; Pinzino, C.; Solmi, M. V.; Zacchini, S. The Redox Chemistry of $[Co_6C(CO)_{15}]^{2-}$: A Synthetic Route to New Co-Carbide Carbonyl Clusters. *Inorg. Chem.* **2014**, *53*, 3818.

55 (a) Ciabatti, I.; Fabrizi de Biani, F.; Femoni, C.; Iapalucci, M. C.; Longoni, G.; Zacchini, S. Metal Segregation in Bimetallic Co-Pd Carbide Carbonyl Clusters: Synthesis, Structure, Reactivity and Electrochemistry of $H_{6-n}Co_{20}Pd_{16}C_4(CO)_{48}]^{n-}$ (n = 3-6) *ChemPlusChem* **2013**, *78*, 1456. (b) Ciabatti, I.; Femoni, C.; Iapalucci, M. C.; Longoni, G.; Zacchini, S.; Fedi, S.; Fabrizi de Biani, F. Synthesis, Structure, and Electrochemistry of the Ni-Au

Carbonyl Cluster $[Ni_{12}Au(CO)_{24}]^{3-}$ and Its Relation to $[Ni_{32}Au_6(CO)_{44}]^{6-}$. *Inorg. Chem.* **2012**, *51*, 11753.

56 Johnson, N. W. Convex polyhedra with regular faces. *Can. J. Math*., 1966, **18**, 169.

57 Mingos, D. M. P.; Wales D. J. *Introduction to cluster Chemistry*. Prentice Hall, Englewood Cliffs, 1990.

58 Vidal, J. L. $[Rh_{10}As(CO)_{22}]^{3-}$. Example of Encapsulation of Arsenic by Transition-Metal Carbonyl Clusters As Illustrated by the Structural Study of the Benzyltriethylammonium Salt. *Inorg. Chem.* **1981**, *20*, 243.

59 Ciani, G.; Garlaschelli, L.; Sironi, A.; Martinengo, S. Synthesis and X-ray characterization of the novel $[Rh_{10}S(CO)_{10}(\mu\text{-}CO)_{12}]^{2-}$ anion; a bicapped square-antiprismatic cluster containing an interstitial sulphur atom. *J. Chem. Soc., Chem. Commun.* **1981**, 536b.

60 (a) Bernardi, A.; Femoni, C.; Iapalucci, M. C.; Longoni, G.; Zacchini, S. The problems of detecting hydrides in metal carbonyl clusters by ^1H NMR: the case study of $[H_{4-n}Ni_{22}(C_2)_4(CO)_{28}(CdBr)_2]^{n-}$ (n = 2-4). *Dalton Trans*. **2009**, 4245. (b) Collini, D.; Fabrizi de Biani, F.; Dolzhnikov, D. S.; Femoni, C.; Iapalucci, M. C.; Longoni, G.; Tiozzo, C.; Zacchini, S.; Zanello, P. Synthesis, Structure, and Spectroscopic Characterization of $[H_{8-n}Rh_{22}(CO)_{35}]^{n-}$ (n = 4,5) and $[H_2Rh_{13}(CO)_{24}\{Cu(MeCN)\}_2]^-$ Clusters: Assessment of CV and DPV As Techniques to Circumstantiate the Presence of Elusive Hydride Atoms. *Inorg. Chem.* **2011**, *50*, 2790. (c) Ciabatti, I.; Femoni, C.; Iapalucci, M. C.; Longoni, G.; Zacchini, S. Tetrahedral $[H_nPt_4(CO)_4(P\text{^}P)_2]^{n+}$ (n = 1, 2; P^P = CH_2=$C(PPh_2)_2$) Cationic Mono- and Dihydrido Carbonyl Clusters Obtained by Protonation of the Neutral $Pt_4(CO)_4(P\text{^}P)_2$. *Organometallics* **2013**, *32*, 5180.

61 Femoni, C.; Iapalucci, M. C.; Longoni, G.; Zacchini, S.; Fedi, S.; Fabrizi de Biani, F. Nickel poly-acetylide carbonyl clusters: structural features, bonding and electrochemical behavior. *Dalton Trans.* **2012**, *41*, 4649.

62 Femoni, C.; Iapalucci, M. C.; Longoni, G.; Tiozzo, C.; Zacchini, S. An Organometallic Approach to Gold Nanoparticles: Synthesis and X-Ray Structure of CO-Protected $Au_{21}Fe_{10}$, $Au_{22}Fe_{12}$, $Au_{28}Fe_{14}$, and $Au_{34}Fe_{14}$ Clusters. *Angew. Chem. Int. Ed.* **2008**, *47*, 6666.

63 Ragaini, F.; Song, J.-S.; Ramage, D. L.; Gregory, L. .; Yap, G. A. P.; Rheingold, A. L. Radical Processes in the Reduction of Nitrobenzene Promoted by Iron Carbonyl Clusters. X-ray Crystal Structures of $[Fe_3(CO)_9(\mu_3\text{-}NPh)]^{2-}$, $[HFe_3(CO)_9(\mu_3\text{-}NPh)]^-$, and the Radical Anion $[Fe_3(CO)_{11}]^{-\bullet}$. *Organometallics* **1995**, *14*, 387.

64 (a) Calabrese, J. C.; Dahl, L. F.; Cavalieri, A.; Chini, P.; Longoni, G.; Martinengo, S. Synthesis and Structure of a Hexanuclear Nickel Carbonyl Dianion, $[Ni_3(CO)_3(\mu_2\text{-}CO)_3]^{2-}$,

and Comparison with the $[Ni_3(CO)_3(\mu_2\text{-}CO)_3]^{2-}$ Dianion. An Unprecedented Case of a Metal Cluster System Possessing Different Metal Architectures for Congener Transition Metals. *J. Am. Chem. Soc.* **1974**, *96*, 2616; (b) Longoni, G.; Chini, P.; Cavalieri, A. Carbonylnickelates 1. Synthesis and Chemical Characterization of the $[Ni_5(CO)_{12}]^{2-}$ and $[Ni_6(CO)_{12}]^{2-}$ Dianions. *Inorg. Chem.* **1976**, *15*, 3025.

65 Keller, E. SCHAKAL99; University of Freiburg: Germany, 1999.

66 Krejčik, M.; Daněk, M.; Hartl, F. Simple construction of an infrared optically transparent thin-layer electrochemical cell: Applications to the redox reactions of ferrocene, $Mn_2(CO)_{10}$ and $Mn(CO)_3$(3,5.di-t-butyl-catecholate)$^-$. *J. Electroanal. Chem*. **1991**, *317*, 179.

67 Sheldrick, G. M. SADABS, Program for empirical absorption correction; University of Göttingen: Germany, 1996.

68 Sheldrick, G. M. Crystal structure refinement with SHELXL. *Acta Crystallogr. C*, **2015**, *71*, 3.

Table of contents

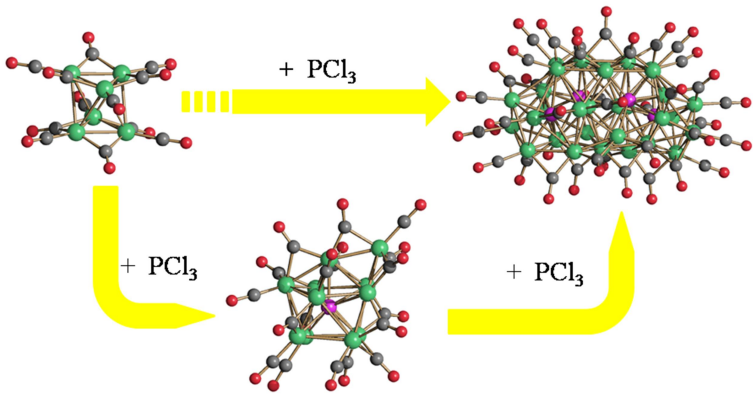

The molecular nickel phosphide carbonyl nanoclusters $[Ni_{11}P(CO)_{18}]^{3-}$ and $[H_{6-n}Ni_{31}P_4(CO)_{39}]^{n-}$ (n = 4,5) were obtained from the reaction of $[Ni_6(CO)_{12}]^{2-}$ with increasing amounts of PCl_3. Their polyhydride nature and redox behavior were investigated by means of electrochemical and spectroelectrochemical studies.